Atmospheric
Chemistry
and Physics
Discussions

Sources and mixing state of summertime background aerosol in the northwestern Mediterranean basin

Jovanna Arndt[1], Jean Sciare[2,3], Marc Mallet[4], Greg C. Roberts[4,5],
Nicolas Marchand[6], Karine Sartelet[7], Karine Sellegri[8], François Dulac[2], Robert
M. Healy[9], and John C. Wenger[1]

[1]Department of Chemistry and Environmental Research Institute, University College Cork, Cork, Ireland
[2]LSCE, Laboratoire des Sciences du Climat et de l'Environnement, Unité Mixte CEA-CNRS-UVSQ, Univ. ParisSaclay, CEA Saclay/Orme des Merisiers 701, F-91191 Gif-sur-Yvette, France
[3]Energy, Environment and Water Research Center, The Cyprus Institute, 2121 Nicosia, Cyprus
[4]CNRM, Centre National de Recherches Météorologiques UMR 3589, Météo-France/CNRS, Toulouse, France
[5]Scripps Institution of Oceanography, Center for Atmospheric Sciences and Physical Oceanography, La Jolla, United States
[6]Aix Marseille Univ, CNRS, LCE, Marseille, France
[7]CEREA, Centre d'Enseignement et de Recherche en Environnement Atmosphérique, Joint Laboratory ENPC ParisTech/EDF R&D, Université Paris-Est, Marne la Vallée, France
[8]LaMP, Laboratoire de Météorologie Physique CNRS UMR6016, Observatoire de Physique du Globe de Clermont-Ferrand, Université Blaise Pascal, Aubière, France
[9]Environmental Monitoring and Reporting Branch, Ontario Ministry of the Environment and Climate Change, Toronto, Canada

Correspondence to: John C. Wenger (j.wenger@ucc.ie)

Abstract. An aerosol time-of-flight mass spectrometer (ATOFMS) was employed to provide real-time single particle mixing state and thereby source information for aerosols impacting the western Mediterranean basin during the ChArMEx-ADRIMED and SAF-MED campaigns in summer 2013. The ATOFMS measurements were made at a ground-based remote site on the northern tip

5 of Corsica Island. 27 distinct ATOFMS particle classes were identified and subsequently grouped into 8 general categories: EC-rich (elemental carbon), K-rich, Na-rich, Amines, OC-rich (organic carbon), V-rich, Fe-rich and Ca-rich. Mass concentrations were reconstructed for the ATOFMS particle classes and found to be in good agreement with other co-located quantitative measurements (PM_1, black carbon (BC), organic carbon, sulfate mass and ammonium mass). Total ATOFMS re-

10 constructed mass ($PM_{2.5}$) accounted for 70-90% of measured PM_{10} mass and was comprised of regionally transported fossil fuel (EC-rich) and biomass burning (K-rich) particles. The accumulation of these transported particles was favoured by repeated and extended periods of air mass stagnation over the western Mediterranean during the sampling campaigns. The single particle mass spectra proved to be valuable source markers, allowing the identification of fossil fuel and biomass burn-

15 ing combustion sources, and therefore highly complementary to quantitative measurements made

Atmospheric
Chemistry
and Physics
Discussions

by particle-into-liquid sampler ion chromatography (PILS-IC) and an aerosol chemical speciation monitor (ACSM), which have demonstrated that PM_1 and PM_{10} were comprised predominantly of sulfate, ammonium and OC. Good temporal agreement was observed between ATOFMS EC-rich and K-rich particle mass concentrations and combined mass concentrations of BC, sulfate, ammonium

20 and low volatility oxygenated organic aerosol (LV-OOA). This combined information suggests that combustion of fossil fuels and biomass produced primary EC- and OC-containing particles, which then accumulated ammonium, sulfate and alkylamines during regional transport. Three other sources were also identified: local biomass burning, marine and shipping. Local combustion particles (emitted in Corsica) contributed little to $PM_{2.5}$ particle number and mass concentrations but were easily

25 distinguished from regional combustion particles. Marine emissions comprised fresh and aged sea salt; the former detected mostly during one 5-day event during which it accounted for 50-80% of sea salt aerosol mass, while the latter detected throughout the sampling period. Dust was not efficiently detected by the ATOFMS, and support measurements showed that it was mainly in the $PM_{2.5-10}$ fraction. Shipping particles, identified using markers for heavy fuel oil combustion, were associated

30 with regional emissions, and represented only a small fraction of $PM_{2.5}$ particle number and mass concentration at the site.

1 Introduction

The atmosphere in the Mediterranean basin is strongly influenced by numerous and varied aerosol sources. Anthropogenic emissions from heavily industrialised parts of Southern Europe (e.g. Genoa

35 and Milan), the megacities of Istanbul and Cairo, a large range of smaller population centres disseminated all over the basin, as well as intense shipping activities render the Mediterranean basin one of the most impacted zones on the planet to air pollution (de la Paz et al., 2013; Karanasiou et al., 2014). Natural sources such as Saharan dust, sea-spray and frequent forest fires exert further considerable stress on regional air quality (Kanakidou et al., 2011). Transport of air pollution

40 from outside the Mediterranean region is one cause for increased concentrations of primary and secondary pollutants (Lelieveld et al., 2002). In the summertime upper troposphere, Asian monsoon outflow transports pollution across northern Africa and the Mediterranean (Scheeren et al., 2003). In the middle troposphere, westerly winds prevail, transporting polluted air masses from western Europe and North America (Marmer and Langmann, 2005). In the surface layer, land emissions from

45 south and central Europe are transported to the eastern Mediterranean by northerly winds (Sciare et al., 2003). The geography and regional meteorological processes in the western Mediterranean also favour the accumulation and ageing of polluted air masses (Gangoiti, 2001; Lelieveld et al., 2002; Millán et al., 2000, 2002; Millán and Salvador, 1997; Rodríguez et al., 2002; Salvador et al., 1999; Soriano et al., 2001). Arid conditions, combined with high solar radiation and photochemical

50 conversion rates significantly enhance air pollution mostly in the form of $PM_{2.5}$ and O_3. The high-

Atmospheric
Chemistry
and Physics
Discussions

est particulate matter (PM) concentrations are generally found in southern and eastern Europe and attributed to diverse emission sources such as industry, traffic, resuspended dust, shipping emissions and African dust intrusions (Karanasiou et al., 2007, 2009, 2011, 2014; Lelieveld et al., 2002; Querol et al., 2004; Rodríguez et al., 2007; Salameh et al., 2015). A number of studies have reported that

55 in rural environments in the Mediterranean, airborne PM and ammonium sulfate concentrations undergo a seasonal cycle characterised by a summer maximum (Bergametti et al., 1989; Kubilay and Saydam, 1995; Querol et al., 1998a, b; Rodríguez et al., 2002). This seasonal cycle has not been reported at rural sites in central and northern Europe, where high PM events are mostly recorded in winter during stagnant episodes caused by cold temperature inversions and low wind speed (Beek-

60 mann et al., 2015; Favez et al., 2007; Monn et al., 1995; Röösli et al., 2001; Turnbull and Harrison, 2000). Long term measurements at sites in the western and eastern Mediterranean basins by Querol et al. (2009) showed that mineral matter is the major component of PM_{10} (22-38%) in both areas, with relatively high proportions in $PM_{2.5}$ (8-14%), followed by sulfate, organic matter (OM), nitrate and ammonium. Most studies to date have documented Mediterranean aerosol properties in

65 the eastern basin or at coastal continent-based sites in the western basin, where they were subject to the proximity of considerable urban or industrial emissions. Land-based measurements of the background composition of western Mediterranean atmospheric aerosol is best investigated on the shore line of relatively industry-free, less urbanised islands and studies in such locations have thus far been limited. One of the central aims of the ChArMEx (Chemistry-Aerosol Mediterranean

70 Experiment; https://charmex.lsce.ipsl.fr) project is to make background aerosol observations in such islands as Corsica and the Balearic Islands. In addition, studies of the chemical composition of single aerosol particles in the Mediterranean are particularly scarce and are restricted to urban environments (Dall'Osto et al., 2013, 2016; Dall'Osto and Harrison, 2006; McGillicuddy, 2014). Single particle mass spectrometers, such as the aerosol time-of-flight mass spectrometer (ATOFMS), have proven

75 valuable in identifying and characterising a wide variety of particle sources; sea salt, mineral dust, vehicle exhaust, tyre wear, solid fuel combustion (coal, peat and wood), shipping and various industrial emissions (Beddows et al., 2004; Bhave et al., 2001, 2002; Dall'Osto et al., 2014; Giorio et al., 2012; Harrison et al., 2012; Healy et al., 2009, 2010, 2012; Liu et al., 2003; Spencer et al., 2008; Tao et al., 2011). Mixing state information – both internal and external – provided by mass spectrome-

80 ters has been used to determine the type of atmospheric processing particles have undergone (Gard et al., 1998), as well as their acidity and hygroscopicity (Denkenberger et al., 2007; Healy et al., 2015), properties which affect their ability to act as CCN (Furutani et al., 2008). Combination of ATOFMS and hygroscopicity tandem differential mobility analyser (HTDMA) data has shown that sea salt and particles containing amines and nitrate are hydrophilic, while the more organic carbon

85 (OC) particles contain the more hydrophobic they are (Herich et al., 2009; Wang et al., 2014). Fresh particles can be distinguished from aged ones by the presence of secondary inorganic species such as nitrate, sulfate and ammonium (Cahill et al., 2012; Healy et al., 2010; Liu et al., 2003; Pratt and

Atmospheric
Chemistry
and Physics
Discussions

Prather, 2009), which is also helpful in differentiating particles from local and transported sources (Healy et al., 2012). Single particle chemical speciation is therefore a useful tool, complementary to

90 characterising particle optical and physical properties (Moffet and Prather, 2009), for examining the effect aerosols have on air quality and climate. Measurements from the ATOFMS also provide useful information to validate mixing-state resolved models (Zhu et al., 2016). In air quality and climate models, mixing-state information is essential as this property strongly impacts aerosol composition, hygroscopicity, optical and CCN properties over urban areas (Zhu et al., 2016). An important

95 application of single-particle data is source apportionment of ambient aerosol. If a unique particle composition signature can be linked with a specific source, then number and mass concentration contributions can be estimated at a receptor site (Allen et al., 2000; Bein et al., 2006; Pratt and Prather, 2009; Qin et al., 2006; Reinard et al., 2007). Most chemical speciation measurements to date in the Mediterranean have focused on bulk aerosol, and while they provide quantitative data

100 they do not resolve the mixing states of ambient particles. As such, source identification and therefore apportionment – often one of the main goals of aerosol measurements – is limited with these techniques. In this context, an aerosol time-of-flight mass spectrometer (ATOFMS) was employed to provide real-time single particle mixing state and thereby source information for aerosols impacting the western Mediterranean basin during two ChArMEx special observation periods in summer 2013:

105 ADRIMED (Aerosol Direct Radiative Impact on the regional climate in the MEDiterranean region; Mallet et al., 2016) and SAF-MED (Secondary Aerosol Formation in the MEDiterranean).

2 Methodology

2.1 Sampling site and instrumentation

Measurements were performed at the atmospheric monitoring station in Ersa (coordinates: 42°58'09"N,

110 09°22'49"E), Cape Corsica, near the North tip of Corsica Island. This station is well positioned to investigate polluted air masses transported over the western Mediterranean basin from the highly industrialised regions of the Po Valley (Royer et al., 2010) and/or Marseille/Fos-Berre (El Haddad et al., 2011, 2013). The site was fully equipped for the measurement of aerosol chemical, physical and optical properties. This ground-based remote station is located at an altitude of 530 m above

115 sea level (asl) at the remote Cape Corsica Peninsula and has unobstructed views to the sea over ~270°(Lambert et al., 2011). The ADRIMED and SAF-MED field campaigns took place from 11th June to 5th July and from 12th July to 6th August 2013, respectively, during the Mediterranean dry season over the western and central Mediterranean basins. Some of the key instruments deployed during the campaigns are given in Table 1. A full list of instruments deployed during ADRIMED

120 can be found in the overview for this campaign by Mallet et al. (2016), while a summary of the main findings of the SAF-MED campaign is currently in preparation. The ATOFMS (TSI model 3800) was operated continuously from 12th June – 6th August, with a period of downtime from 12-18th July. A

detailed description of the ATOFMS can be found elsewhere (Gard et al., 1997). Briefly, it consists
of (i) an aerodynamic focussing lens (TSI AFL100) Su et al. (2004) that transmits particles in the
aerodynamic diameter (D_a) range 100-3000 nm, (ii) a particle sizing region, and (iii) a bipolar reflec-
tron time-offlight mass spectrometer. Single particles are desorbed/ionized using a pulsed Nd:YAG
laser (λ = 266 nm, ~1 mJ pulse^{-1}). Positive and negative ion mass spectra of individual aerosol par-
ticles are obtained, which enable identification of the chemical constituents. Gradual degradation in
the power of the sizing lasers during the campaign was observed and resulted in effective size ranges
of 300-3000 nm D_a for ADRIMED and 500-3000 nm D_a for SAF-MED.

2.2 ATOFMS Data Analysis

Over 1.2 million single particle mass spectra were generated by the ATOFMS during the sampling
period and clustered using the K-means algorithm (K=80), as described in detail elsewhere (Gross
et al., 2010; Healy et al., 2009, 2010). Clusters exhibiting very similar average mass spectra (in-
cluding those with the same major ions but varying relative signal intensities), comparable temporal
trends and size distributions were merged. The final merged clusters were then identified as particle
"classes"; 27 in total.

The particle class labelling scheme used herein is regularly used in the literature (Ault et al., 2010;
Dall'Osto and Harrison, 2006; Pratt and Prather, 2012; Spencer and Prather, 2006) and indicates
either the probable source (e.g. sea salt) or the dominant species in the positive ion mass spectra
(e.g. K, EC, Fe etc.), with the order of the ions indicating their relative mass spectral intensities. For
example, a particle class with high intensity mass spectral features for sodium and elemental carbon
is labelled *Na-EC*. In some cases this is followed by a secondary species detected in the negative
mass spectra (e.g. *K-NO$_X$*), which usually provides insight into the atmospheric ageing the particles
have undergone locally or during transport (Reinard et al., 2007).

Single-particle mass spectrometers such as the ATOFMS do not provide quantitative information
in the form of particle number or mass concentrations – rather the ATOFMS provides speciation in
particle counts classified by aerodynamic diameter. The transmission biases of the AFL, the number
of particles the system can size and ionise at any given time (data acquisition busy time), as well as
limited detection of particles <150 nm (determined by wavelength of sizing lasers and the amount
of scattered light) hinder full and accurate counting of particles over the entire ATOFMS size range
(100-3000 nm D_a). The desorption/ionisation laser used by the ATOFMS also complicates quan-
titative speciation. Shot-to-shot fluctuations in laser output power and variations in power density
(Gaussian) across the laser beam (Steele et al., 2005; Wenzel and Prather, 2004) create variance in
the amount of a particle that is desorbed and can also lead to variations in resultant mass spectral
peak height and area (Reinard and Johnston, 2008).

Given these limitations, in order to produce meaningful particle number and mass concentra-
tions for ATOFMS particle classes the total ATOFMS counts were scaled using quantitative particle

Atmospheric
Chemistry
and Physics
Discussions

Open Access

counting instruments operated concurrently; an optical particle counter (OPC, TSI model 3300) and
160 a scanning mobility particle sizer (SMPS, TSI DMA model 3080 and CPC model 3010). Reconcil-
ing SMPS, OPS and ATOFMS data requires conversion of D_m (electrical mobility diameter; SMPS)
and D_o (optical diameter; OPC) measured with the SMPS and OPS into the corresponding ATOFMS
D_a (aerodynamic diameter), using the following relationship:

$$D_a = \frac{\rho_p D_{ve}}{\rho_0 \chi}$$

165 Where ρ_p is the particle density (discussed hereafter), D_{ve} is the volume equivalent diameter (op-
erationally equivalent to D_m or D_o), ρ_0 is standard density (1 g/cm^{-3}) and χ is the dynamic shape
factor (assumed to be 1, thus representing spherical shape). This is a simplified version of particle
diameter, morphology and density relationships that are covered in much greater detail elsewhere
(DeCarlo et al., 2004). No correction factors were used to merge the SMPS and OPS data; D_m and
170 D_o were both assumed to be equivalent to geometric diameter.

Knowledge of particle density is required for this conversion. This value can be estimated from
bulk mass concentration measurements made, for example, by an aerosol chemical speciation moni-
tor (ACSM) and an instrument which measures black carbon (BC), such as a multi-angle absorption
spectrometer (MAAP).

175 $$\textit{Average density} = \frac{m_{BC} + m_{org} + m_{Cl} + m_{SO_4} + m_{NO_3} + m_{NH_4}}{\frac{m_{BC}}{1.5} + \frac{m_{org}}{1.2} + \frac{m_{Cl}}{1.5} + \frac{m_{SO_4} + m_{NO_3} + m_{NH_4}}{1.5}}$$

2.3 Correlations

Reconstructed ATOFMS mass concentrations were then compared, using regression analysis and
the coefficient of determination, with those obtained by the TEOM (tapering element oscillating
microbalance; PM_{10} and PM_1 mass concentrations), PILS-IC (PM_{10} mass concentrations of SO_4^{2-},
180 NH_4^+, NO_3^-, K^+, Ca_2^+, Na^+, Mg^+, Cl^-, oxalate, methanesulfonate – MSA), MAAP (BC mass con-
centrations) and ACSM (PM_1 mass concentrations of SO_4^{2-}, NH_4^+, NO_3^-, Cl^-, organic carbon).
Positive matrix factorisation (PMF) performed on the ACSM organic fragments produces factors
which correspond to a group of OA constituents with similar chemical composition and temporal
behaviour that are characteristic of different sources and/or atmospheric processes (Zhang et al.,
185 2011). Three factors were resolved; low-volatility oxygenated organic aerosol (LV-OOA, aged and
non-volatile), semi-volatile oxygenated organic aerosol (SV-OOA, less oxidised and aged than LV-
OOA) and hydrocarbon-like organic aerosol (HOA, representative of fossil fuel combustion). More
information on ACSM results and source apportionment are available in Michoud et al. (2016).

The coefficient of determination, as R^2, was used to evaluate the effectiveness of the ATOFMS
190 mass reconstruction. All R^2 values can be found in SI Table 1. This analysis was considered ap-
propriate as the objective of ATOFMS mass reconstruction was to produce mass concentrations as
similar as possible to other mass measurement techniques. R^2 values of <0.5, ~0.5-0.7 and >0.7 are

Atmospheric
Chemistry
and Physics
Discussions

typically considered indicative of weak, moderate and strong linear (positive or negative) relationships respectively.

3 Results and Discussion

3.1 Air mass back trajectories

Back trajectory analysis was performed using the HYSPLIT model (Revision 631, July 2014) (Draxler and Hess, 1998) to identify air masses influencing the sampling site. The HYSPLIT model was run using the PC Windows based software available online (http://www.ready.noaa.gov/HYSPLIT.php) and meteorological input from the Global Data Assimilation System (GDAS) archive. 120-hour back trajectories ending 500 m above ground level (AGL) at Ersa (Corsica) were calculated for each hour between 12th June and 7th August 2013 (total: 1344 trajectories). Five broad periods with different air mass regimes were identified in the period based on the ATOFMS, OPS, ACSM, PM_1 and PM_{10} temporal profiles. Separate cluster analyses were performed to classify the trajectories for each of these five campaign periods (Figure 1). A plot of total spatial variance as a function of the number of clusters was used to determine the number of clusters. The clustered HYSPLIT 120-hr back trajectories for each period were used to determine which air masses most influenced the ATOFMS measurements, and temporal profiles for particle numbers and mass concentrations have been labelled with these air mass origins (France, Mediterranean, Spain, North Atlantic, UK, Italy, eastern Europe).

Period 1 (12-20th June) was dominated by recirculating air masses over the Mediterranean Sea, Period 2 (20-26th June) by North Atlantic air masses, Period 3 (26th June-4th July) by trajectories passing largely over France, Period 4 (4-29th July) mostly by Mediterranean recirculations, and Period 5 (29th July-7th August) by Mediterranean recirculations and continental European air masses. The sampling site was therefore influenced by long-range North Atlantic marine emissions and European emissions which were subsequently recirculated over the Mediterranean Sea, with relatively infrequent input from the Sahara. Combined with a sampling period of 8 weeks, it is clear that the site was well placed to provide an insight into the composition of Mediterranean aerosol from diverse sources under a wide variety of meteorological conditions.

3.2 ATOFMS particle classes

Twenty-seven distinct ATOFMS particle classes were identified and subsequently grouped into 8 general "categories" for clarity based on the dominant marker ions; EC-rich (53% of total mass spectra), K-rich (32%), Na-rich (8%), Amines (4%), OC-rich (2%), V-rich (1%), Fe-rich (0.2%) and Ca-rich (0.2%). The contribution to total particle number and mass concentration of all particle classes can be found in Table 2.

Atmospheric
Chemistry
and Physics
Discussions

While the aerosol mixing state is varied, only a few particle classes represent the bulk of un-scaled particle numbers. The dominant classes are *EC-SO$_X$*, *K-SO$_X$* and *K-EC-Oxalate*. The Na-rich category is dominated by *Sea salt-aged* particles, the EC-rich category by *EC-SO$_X$* particles, the K-rich category by *K-SO$_X$* particles, the Amines category by *K-TMA* and *EC-TMA* particles, the
230 OC-containing category by *OC* particles and the V-rich category by *V* particles.

3.3 Mass Concentrations

Reconstructed ATOFMS mass concentrations were compared with those for PM$_{10}$, total PILS-IC species (PM$_{10}$) and PM$_1$ (total ACSM species + BC), shown in Figure 2. Reconstructed ATOFMS particulate mass accounted for 70-90% of PM$_{10}$ mass for most of the sampling period. Note that
235 ATOFMS particles account for relatively little of the PM$_{10}$ mass during periods when sea salt and dust are abundant, which is expected given the upper size limit (3 μm) of the instrument and the low detection efficiency for supermicron particles (Cahill et al., 2014). Total ATOFMS reconstructed mass concentrations were found to correlate well with total ACSM mass concentrations (R^2 =0.71), and moderately with mass concentrations of PILS-IC SO$_4^{2-}$ and NH$_4^+$ (R^2 =0.58, 0.44), the ACSM
240 factors LV-OOA (R^2 =0.59) and SV-OOA (R^2 =0.46), BC (R^2 =0.55) and PM$_1$ (R^2 =0.44).

ATOFMS reconstructed mass concentrations were dominated by EC-rich particles (52%), followed by K-rich (25%), Na-rich (12%), Amines (3%), OC-rich (3%), V-rich (3%), Ca-rich (1%) and Fe-rich (1%). The dominance of EC and K-rich ATOFMS particles does not suggest that PM$_{2.5}$ mass is comprised mostly of EC and K. These species are simply used as markers (and for naming
245 conventions) in ATOFMS analysis for fossil fuel and biomass combustion, while truly quantitative measurements by the PILS-IC and ACSM indicate that most of the PM$_{10}$ mass was comprised of organics (36%), sulfate (16%) and ammonium (10%). A detailed discussion follows in Section 3.4.1.

3.4 Particle Sources

Four general sources of ATOFMS PM$_{2.5}$ particles were identified during ADRIMED and SAF-MED,
250 namely regionally transported combustion, local biomass burning, marine, and shipping. Composition of the particle classes that may have originated from these sources, and comparison of their mass concentrations with other measurements is discussed in the following sections.

3.4.1 Regionally Transported Combustion

Twelve ATOFMS particles classes were identified as originating from regionally transported com-
255 bustion, all found in the following 3 categories; EC-rich, K-rich and Amines. Average mass spectra for these particles classes are shown in Figure 3. All of the EC-rich classes were characterised by elemental carbon fragments ions $^{12,24,36\cdots}$C$^+$ in the positive mass spectra. *EC-SO$_X$* and *EC-Oxalate* did not contain detectable ^{39}K$^+$, indicating they most likely arise from fossil fuel combustion (oil burning or traffic). *EC-K*, *EC-K*-SO$_X$ and *EC-K*-Oxalate were characterised by a stronger signal

260   for $^{36}C_3^+$ relative to $^{39}K^+$; similar particles have previously been attributed to domestic coal com-
bustion (Healy et al., 2010), although other sources are certainly possible. *K-EC-NO$_X$*, *K-EC-SO$_X$*
and *K-EC-Oxalate* produced stronger signals for $^{39}K^+$ relative to $^{36}C_3^+$, a pattern usually associ-
ated with biomass burning particles. Sulfate ($^{97}HSO_4H^-$) dominated the SO$_X$ classes, but was also
present to a lesser extent in the other six EC-rich classes. Despite the average spectra for the EC-rich

265   classes showing large signals for sulfate and nitrate ($^{46}NO_2^-$, $^{62}NO_3^-$) most of the particles in these
classes produced no negative ion spectra or only weak negative ion signals. It is therefore not possi-
ble to definitively describe their anion mixing state; however certain conclusions can still be drawn
from their temporal profiles. Less nitrate, or weaker signals for these species, relative to sulfate was
expected given the high ambient temperatures; nitrate is usually mixed with EC in the form of am-

270   monium nitrate, which is more volatile than ammonium sulfate (Querol et al., 2009; Sciare et al.,
2008). A smaller signal for MSA, $^{95}(CH_3)SO_3^-$ (Neubauer et al., 1997), relative to sulfate was found
in the *K-EC-SO$_X$* class, indicating processing with marine emissions (Gaston et al., 2010). The ox-
alate classes are characterised by their signal at m/z -89, a marker for deprotonated oxalic acid (Yang
et al., 2009) and aged aerosol. Very small signals for ammonium ($^{18}NH_4^+$), not marked in the mass

275   spectra, were found in all classes with the exception of the *EC-Oxalate* class.

The positive ion mass spectra for *K-CN* and *K-SO$_X$* particles are exclusively dominated by $^{39}K^+$,
typical of biomass burning particles detected by ATOFMS (a.R. Lea-Langton et al., 2015; Pratt
et al., 2010; Qin and Prather, 2006; Silva et al., 1999). Sulfate ($^{97}HSO_4H^-$) dominates the negative
ion mass spectra of the *K-SO$_X$* particles, with additional signals for MSA ($^{95}(CH_3)SO_3^-$) and ox-

280   alate ($^{89}(COO)_2H^-$). $^{26}CN^-$, internally mixed carbon and nitrogen, probably in the form of nitrogen-
containing organic compounds (Silva et al., 1999), dominates the negative ion mass spectra of *K-CN*
particles. EC fragments were found in all K-rich negative ion mass spectra, indicating a biomass
combustion source.

Trimethylamine (TMA, $^{59}(CH_3)_3N^+$,) was the most abundant alkylamine marker ion in the three

285   Amine particle classes. Also present in all three classes was a marker ion for protonated dimethy-
lamine (DMA, $^{46}(CH_3)_2NH_2^+$). A comparison of ATOFMS datasets obtained in Cork, Paris, Zurich,
Dunkirk and Corsica (ADRIMED and SAFMED) found this ion only in the latter two datasets (Healy
et al., 2015). Ammonium ($^{18}NH_4^+$) was also found in all three Amine classes. The *K-TMA* class was
dominated by $^{39}K^+$, indicative of biomass burning, while *EC-TMA* particles produced $^{12,36}C_3^+$ sig-

290   nals, indicating fossil fuel combustion origins. *OC-TMA* particles are characterised by strong $^{39,41}K^+$,
OC ($^{27}C_2H_3^+$) and oxidised OC ($^{43}C_2H_3O^+$) signals, suggesting biomass burning sources and atmo-
spheric processing during transport to the site. Sulfate ($^{97}HSO_4H^-$) and nitrate ($^{46}NO_2^-$, $^{62}NO_3^-$,
$^{125}(NO_3)_2^-$) were found in the average negative mass spectra of *EC-TMA* and *OC-TMA*, however
only 0.3% and 18% of these particles actually produced negative mass spectra and *K-TMA* parti-

295   cles produced none. Alkylaminium sulfate particles have been shown to readily absorb water at low
relative humidities (<45%) (Chan and Chan, 2013; Hu et al., 2014), and particle-bound water has

Atmospheric
Chemistry
and Physics
Discussions

been shown to suppress negative ion formation in mass spectrometers (Neubauer et al., 1997, 1998). The proportion of Amine particles with negative mass spectra is low, in contrast to other particle classes which produced signals in up to 100% of their negative mass spectra (K-EC-SO_X, K-SO_X-
300   $Oxalate$). This suggests particle-bound water could have had a significant effect on negative ion formation for these particles. The average negative mass spectra should therefore not be considered as representative of every particle in these classes. Healy et al. (2015) previously assigned m/z -95 in amine-containing particles from this dataset to MSA. However, closer inspection of individual spectra suggests that at least some of the signal at -95 arises from miscalibrated negative ion mass spectra,
305   and is in fact associated with sulfate. Although m/z -95 cannot therefore be definitively assigned to MSA here, internal mixing of MSA and TMA is possible, as indicated by laboratory studies (Chen et al., 2015a). Furthermore, MSA was also measured in bulk PM_{10} during this campaign using the PILS-IC instrument, and is thus inevitably contained in a fraction of particles at this location. Temporal profiles for hourly summed particle numbers for the regionally transported combustion classes
310   are shown in Figure 4. There are three general temporal profiles; those of EC-SO_X, EC-K-SO_X, EC-K and EC-$Oxalate$, those of K-SO_X, K-EC-SO_X, K-CN and K-EC-$Oxalate$, and finally those containing TMA. The EC-rich particle classes dominated Period 1 and were considered markers for fossil fuel combustion because most of these did not contain detectable $^{39}K^+$. Their particle numbers remained relatively similar throughout the campaigns. For the first half of Period 1 regional air masses passed
315   over industrialised parts of France (Marseille) and Northern Italy (Po Valley) before reaching the site, while during the latter half of this period these air masses were then recirculated over the western Mediterranean (SI Figure 1 shows the air mass back trajectories calculated for this period using the HYSPLIT model).

    Particle numbers for all EC-rich and major K-rich classes decreased noticeably during Periods 2
320   and 5, which were influenced by synoptic scale air masses from the North Atlantic, effectively removing aerosol accumulated during the previous periods. On the other hand, K-rich particles, markers for biomass combustion, dominated Periods 3 and 4. Fires were detected by MODIS (Figure 5) over northern Italy, Ukraine and Russia throughout the sampling period and the site was heavily influenced by air masses passing over this region (Figure 1), which could explain the constant presence
325   of K-rich particles in the background aerosol. The increase in these particles during Period 3 may be explained by longer residence times of air masses over southern France and northern Italy relative to Period 1, and particle numbers then began to decrease when trajectories from the North Atlantic and UK arrived at the end of Period 3.

    A significant increase in fires was detected around the Black Sea from 10th July until the end of
330   the sampling period (Figure 5). The burning of wheat residuals has been previously documented in the eastern Mediterranean and contributed at least 30% of EC and OC measured during similar time periods between 2001-2006 (Sciare et al., 2008). For ~4 days during Period 4, air masses from over the Black Sea and eastern Europe influenced the site, followed by extensive stagnation and

Atmospheric
Chemistry
and Physics
Discussions

recirculation of that air over the western Mediterranean. These observations coincided with a further

335 increase in K-rich particle numbers relative to Period 3.

As shown in Figure 4, the three Amine particles classes, *K-TMA*, *EC-TMA* and *OC-TMA*, presented similar temporal profiles in Period 4 to those of major EC-rich and K-rich particles classes. Numbers of *K-TMA* and *EC-TMA* particles peaked during Period 4, while *K-TMA* particles dominated over *EC-TMA* particles during Period 3, as was the case for the major K-rich and EC-rich

340 classes. The dominant Amine class, *K-TMA*, correlated well with two major classes, *K-SO$_X$* and *K-EC-Oxalate*, particularly during Period 4 (R^2=0.76, 0.70 respectively). Partitioning of alkylamines from the gas phase to particles has been found to be enhanced during periods of high relative humidity or fog events, with uptake increasing with aerosol acidity Rehbein et al. (2011). No association between any of the Amine classes and local relative humidity was found in this case, suggesting that

345 this effect is not relevant close to the site but may have played a role close to the point of emission or during transport of the Amine particles to the site. It also provides further evidence that the Amine particles were not formed in the local environment.

To investigate how the dominant ATOFMS particle categories (EC and K-rich) compared with the dominant bulk PM$_{10}$ (excluding sea salt) species, hourly mass concentrations of PM$_{10}$, BC, ACSM

350 species (SO$_4^{2-}$, NH$_4^+$ and SVOOA) and reconstructed mass concentrations for ATOFMS EC-rich and K-rich particle categories (combined particle classes) were plotted (Figure 6). EC and K-rich mass concentrations have been stacked to compare their values with the contributions from BC, SV-OOA, LV-OOA, SO$_4^{2-}$ and NH$_4^+$ (also stacked). For the full sampling period reconstructed mass concentrations of all ATOFMS EC-rich particle classes correlated well with ACSM SO$_4^{2-}$ (R^2=0.61),

355 NH$_4^+$ (R^2=0.62) and the LV-OOA factor (R^2=0.59) mass concentrations (which accounted for the largest proportion of organics mass, 54%), OPS (for the channel 0.3-0.579 μm) number concentrations (R^2=0.69) and moderately with PM$_1$ (R^2=0.46) and BC (R^2=0.50) mass concentrations. Reconstructed mass concentrations for all K-rich classes (including local combustion) correlated with the same species but only moderately (R^2 ranged from 0.3-0.5). Individual particle classes did

360 not produce stronger correlations, suggesting that no single class was an important contributor of PM$_{2.5}$ composition.

The average mass spectra of ATOFMS EC and K-rich classes showed sulfate, nitrate, oxalate and MSA were present. From the PILS-IC and ACSM measurements it was clear that the dominant secondary inorganic ions were sulfate (19% of PM$_1$, 16% of PM$_{10}$) and ammonium (10% of PM$_1$,

365 10% of PM$_{10}$), with nitrate contributing relatively little to both PM$_1$ (4%) and PM$_{10}$ (4%) mass. K$^+$, oxalate and MSA contributed less again to PM$_{10}$ (0.4, 0.1 and 0.2% respectively). K$^+$ is readily ionised by the ATOFMS desorption/ionisation laser so its prevalence in ATOFMS particles is not necessarily representative of its mass concentration (Gross et al., 2000a).

The high level of agreement between mass concentrations of EC-rich+K-rich particles and BC+SV-

370 OOA+LVOOA+SO$_4^{2-}$+NH$_4^+$, shown in a scatter plot in Figure 6, suggests those particles were com-

prised to a considerable degree of LV-OOA, consistent with the ageing of the aerosol particles during regional transport, and SV-OOA, which suggests interaction with locally formed organic aerosol; details of organic aerosol formation and sources during the campaigns can be found in Michoud et al. (2016). However, no significant OC signals were found in any of the EC-rich or K-rich classes. Par-

375   ticles which did produce strong signals for OC ions contributed relatively little to total ATOFMS particle numbers. Similarly to ^{39}K$^+$, the ATOFMS favours ionisation of EC over OC (Ferge et al., 2006; Silva and Prather, 2000), which results in weak signals for OC in particles which also contain EC or K$^+$. This may account for the under-representation of organic aerosol in the ATOFMS measurements.

380   **3.4.2   Local biomass burning**

The sampling site on Corsica was chosen for its negligible local anthropogenic sources relative to the regional background. However, few local sources did influence the site, though these did not contribute significantly to particle number or mass concentrations. Local combustion events were detected in the form of *K-NO$_X$*, K-OCNOX, and *K-OC-SO$_X$* particles, and distinguished themselves

385   from the dominating regional aerosol by occurring mostly during Periods 1 and 2 over 5-7 hour events (Figure 7). The first event was observed on the 12th June from 13:00-18:00 UTC and its source as biomass burning (in the form of vegetation trimmings) was visually confirmed on the slopes northeast of the site.

The composition of these particles is consistent with this observation; K$^+$ is a common marker

390   for biomass combustion, which typically also produces organic aerosol (Pagels et al., 2013; Silva et al., 1999). Average mass spectra for local biomass burning particles are shown in Figure 8. Nitrate (^{46}NO$_2$$^-$, ^{62}NO$_3$$^-$) dominated the negative mass spectra of *K-NO$_X$* particles, but they also contained sulfate (^{97}HSO$_4$H$^-$), nitrogen-containing organic compounds (^{26}CN$^-$), EC (^{24,36,48}C$^-$) and oxygen (^{16}O$^-$). *K-OC-NO$_X$* and *K-OC-SO$_X$* are characterised by a large signal for ^{39}K$^+$ (confirmed by

395   the prominent signal for the ^{41}K$^+$ isotope, hydrocarbon fragments (^{27}C$_2$H$_3$$^+$, ^{29}C$_2H_5$$^+$, ^{51}C$_4H_3$$^+$, ^{63}C$_5H_3$$^+$) in the positive mode and strong signals for ^{43}C$_2$H$_3$O$^+$, a marker for oxidised organic aerosol (Silva and Prather, 2000). Sulfate was found in both OC-rich classes, but dominated the negative mass spectra of *K-OC-SO$_X$* particles. *K-OC-SO$_X$* particles also exhibited a small MSA (^{95}(CH)$_3$SO$_3$$^-$) signal, indicating at least some mixing with marine biogenic emissions prior to detec-

400   tion. Nitrate dominated the *K-OC-NO$_X$* class and was also present to a lesser extent in the *K-OC-SO$_X$* classes.

Garden waste biomass was frequently burned in the surrounding villages during June; such combustion was prohibited from July onwards which explains the lack of similar local events. No local wildfires or controlled agricultural burning was noted during the sampling period. Between 27th June

405   and 1st July, *K-NO$_X$*, *K-EC-NO$_X$* and possibly *K-OC-SO$_X$* were of regional biomass burning origin, because their temporality was noticeably different to the preceding short local events; this period

Atmospheric
Chemistry
and Physics
Discussions

was influenced by short-range air masses residing over southern France and northern Italy. Peak aerodynamic diameters for these particles were also larger during this period compared to previous local combustion events; 700-900 nm (D_a) versus 300-500 nm. This represents a significant amount

410 of growth through ageing, assuming these particles were of a similar size at their point of origin to those burned locally in Corsica. *K-NO$_X$* and *K-OC-SO$_X$* particles were also present throughout both campaigns, in low numbers outside of events, indicating persistent regional sources.

3.4.3 Sea Salt

ATOFMS sea salt particles were separated into two classes; fresh and aged. Their composition and

415 comparison with other sea salt measurements (e.g. Na and Cl mass concentrations from PILS-IC) are the subject of a detailed study of primary marine aerosols during ADRIMED (Claeys et al. 2016), so will only be discussed briefly here. Both sea salt classes are typical of those observed in other coastal/marine environments (Gard et al., 1998; Dall'Osto et al., 2004; Healy et al., 2010). Average mass spectra are shown in Figure 8. The positive modes for both fresh and aged particles are

420 similar and are characterised by sodium ions ($^{23}Na^+$, $^{46}Na_2^+$, $^{62}Na_2O^+$, $^{63}Na_2OH^+$ and $^{81,83}Na_2Cl^+$) and $^{39}K^+$. Fresh and aged sea salt particles were differentiated by their negative mass spectra, which showed peaks for $^{16}O^-$, $^{35,37}Cl^-$, nitrate ($^{46}NO_2^-$, $^{62}NO_3^-$) and $^{93,95}NaCl_2^-$ for fresh sea salt particles, while the signals for nitrate dominate the aged sea salt negative mode and sodium chloride adducts are virtually absent. The absence of NaCl ions and strong nitrate signals indicates extensive replace-

425 ment of Cl^- by NO_3^- (Gard et al., 1998), while the presence of nitrate in the negative mass spectra of the fresh sea salt particles suggests that these are not truly fresh but have also undergone some Cl replacement.

Temporal profiles for ATOFMS sea salt particle numbers, OPS number concentrations, PILS-IC sea salt aerosol (SSA, calculated using SSA=[Cl$^-$]+[Na+]×1.47; Bates et al., 2012) and ATOFMS

430 fresh sea salt mass concentrations are shown in Figure 9. The two ATOFMS sea salt classes presented noticeably different temporal profiles. Aged sea salt was present consistently in the background throughout both campaigns, while fresh sea salt was detected mostly during short periods (20-26th June, 30th July). This coincided with increases in OPS number concentrations in the 0.579-2.156 µm range and PILS-IC SSA. Correlation between ATOFMS fresh sea salt mass and SSA is

435 particularly strong (R^2=0.81) for the sea salt event during Period 2. Reconstructed mass concentrations for fresh sea salt particles accounted for 50-80% of SSA during the main event. This and a strong correlation between ATOFMS fresh sea salt mass concentrations and 0.579-2.156 µm particles (R^2=0.81) suggests a significant amount of fresh sea salt was in the PM$_{2.5}$ fraction; an estimated 30% of PM$_{10}$ SSA mass was accounted for by PM$_{2.5}$ ATOFMS fresh sea salt during the 5-day event

440 in Period 2.

Atmospheric
Chemistry
and Physics
Discussions

3.4.4 Mineral Dust

Three prominent mineral dust events were characterised by increases in Ca_2^+ mass concentrations and 2.156-8.032 μm particle number concentrations during 12-13th June, 17-19th June and 23-26th June (Figure 9). The third event coincided with the main sea salt event and was also distinguished by contributions of K^+. The 17-19th June event is likely related to a moderate African dust event that passed over Corsica, as shown by MSG\SEVIRI aerosol optical depth (SI Figure 2). The two other periods appear due to local dust. Two particle classes were identified as potential mineral dust by the ATOFMS; Fe and Ca. Average mass spectra are shown in Figure 8. Fe and Ca, along with Al and aluminosilicates are typical dust tracers which produce ions detectable by ATOFMS (Guazzotti et al., 2001; Silva et al., 2000; Sullivan et al., 2007).

K-rich dust is also a possibility. The Fe particles detected in Corsica were internally mixed with $^{39}K^+$, $^{23}Na^+$, $^{27}Al^+$, sulfate ($^{97}HSO_4H^-$) and nitrate, although only a weak signal for $^{27}Al^+$ and no aluminosilicate signals (e.g. $^{43}AlO^-$, $^{59}AlO_2^-$, $^{60}SiO_2^-$, $^{76}SiO_3^-$, $^{77}HSiO_3^-$, $^{103}AlSiO_3^-$) were found, which could also suggest industrial origins (Corbin et al., 2012; Dall'Osto et al., 2008; Zhang et al., 2009). Ca particles are dominated by $^{40}Ca^+$, with weaker signals for $^{56}CaO^+$ and $^{96}CaO_2^+$. 34% of all Ca particles produced positive EC ions, which suggests a vehicular traffic source (Gross et al., 2000b; Silva and Prather, 1997; Song et al., 2001) to and from the site and from a few local villages whose tourist population increases during the summer.

The Fe and Ca classes only contributed a small number of particles (0.2% each) relative to the total number ionised by the ATOFMS and no agreement between these potential dust particles and PILS-IC or OPS measurements was found. This indicates that mineral dust was not characterised well by the ATOFMS. Indeed, the dust particle mass-size distribution is mainly in the $>PM_{2.5}$ fraction, but submicron particles dominate the dust particle number size distribution (see Guieu et al., 2010)(Gomes et al., 1990) as confirmed by in situ and column-integrated particle size distribution measurements during the campaign (Denjean et al., 2016; Renard et al., 2016).

3.4.5 Shipping

Two V-rich particle classes (*V* and *EC-V*, 2% and 1% of ATOFMS mass respectively) were identified as originating from heavy fuel oil combustion; both contained $^{51}V^+$, $^{67}VO^+$, $^{56}Fe^+$, $^{58}Ni^+$ and sulfate ($^{97}HSO_4H^-$), which are typical markers for particles emitted by ships or oil refineries (Ault et al., 2009; Healy et al., 2009). A small signal for MSA ($^{95}(CH)_3SO_3^-$) was present in *EC-V* particles. Internally mixed sodium, potassium, calcium, vanadium, nickel and iron particles have also been observed in ship exhaust particles using off-line TEM-EDX and two-step laser mass spectrometry (L2MS) (Moldanová et al., 2009). Small signals for $^{39}K^+$ and $^{23}Na^+$ were found in the Corsica V-rich particles, but none for $^{40}Ca^+$. Heavy fuel oil combustion aerosols have a strong presence in the Mediterranean (Becagli et al., 2016; Pey et al., 2010; Querol et al., 2009). There are more than 15

Atmospheric
Chemistry
and Physics
Discussions

passenger ferry lanes incurring shipping traffic around the northern tip of the island; the closest pass is 16.5 km north and 12.5 km east of the site (Figure 10). Ferries travelling around the northern tip of Corsica Island, take approx. one hour to reach Bastia and between all five ferry companies ~50 sailings take place per week. Both V-rich classes displayed strong north-westerly and southwesterly

480   wind dependences (Figure 10), consistent with the distribution of most ferry lanes (Figure 10) V-rich particles were identified as aged regional emissions. Most freshly emitted shipping particles are typically less than 300 nm D_a (Healy et al., 2009). However, all shipping particles detected during this campaign had diameters larger than 300 nm D_a. Furthermore, it was unlikely that any fresh heavy oil combustion emissions were observed with the ATOFMS as the closest ferry lane is at least

485   12.5 km from the site. There are also no local power plants or refineries that could generate similar particles. *EC-V* and *V* particle numbers consistently featured a mode around 740 nm D_a indicating that the observed particles were aged to some degree.

3.5   Aged Particle Markers

As a substantial number of ionised ATOFMS particles produced low intensity signals in their neg-

490   ative ion mass spectra, or none at all, the average mass spectra are most representative of those species that ionised most efficiently i.e. nitrate and sulfate. Ions that usually produce relatively small signals, such as oxalate or MSA, were expected to be under-represented in the average mass spectra so an additional querying approach was taken to examine the mixing state of these species; particle numbers for classes found to contain these species are shown in Table 2. Oxalate ($^{89}(COO)_2H^-$) and

495   MSA ($^{95}(CH)_3SO_3^-$) ions were queried for peak height between 1 and 5000, to include all mass spectra containing these species. These particles were then clustered using the K-means algorithm to produce particle classes.

3.5.1   Oxalate

The mixing states of particles containing oxalate as identified by single particle techniques is var-

500   ied, and indicates oxalate formation either in fog/cloud processing or photochemical oxidation of biogenic and anthropogenic VOCs. Oxalate has been found in biomass burning particles (Healy et al., 2010; Yang et al., 2009), mixed with industrial combustion particles containing Pb and Zn (Moffet et al., 2008)(Moffet et al., 2008a, 2008b), in aged sea salt (Yang et al., 2009) and in aged carbonaceous particles containing highly oxidised organics, non-oxygenated organics and amines

505   (Pratt et al., 2009; Qin et al., 2012). Oxalic acid has been found preferentially enriched on Asian mineral dust over carbonaceous particles (Sullivan and Prather, 2007), while Fitzgerald et al. (2015) characterised cloud processed African dust as rich in sulfate and oxalate.

In our study, oxalate was found in ~9600 particles, i.e. 0.8% of the total particles ionised. The mixing states derived from this query are similar to those produced from general clustering and

Atmospheric
Chemistry
and Physics
Discussions

510 are varied, suggesting that poor ionisation efficiency did not prevent oxalate from being detected in
certain types of particles.

From the querying approach it was apparent that K-rich particles produced more signals for ox-
alate than the more abundant carbonaceous particles. This could indicate preferential partitioning
to K-rich particles or more extensive oxidation of the OC in those particles versus EC-rich ones.

515 52% of the queried oxalate particles were dominated by $^{39}K^+$ and sulfate (~90% of all the queried
particles contained sulfate), supporting the identification of the *K-SO$_X$-Oxalate* class from the gen-
eral approach. Particles most similar to *K-NO$_X$* accounted for a further 33% and produced signals
for nitrate, EC, CN, CNO and sulfate. In contrast only 2% of queried oxalate particles produced
EC-rich positive mass spectra. Particles with typical dust tracers (Fe, Ca, Al, aluminosilicates) ac-

520 counted for 7% of the queried particles; this fraction applies to PM$_{2.5}$ but would certainly be larger
for PM$_{10}$. The remaining queried oxalate particles were classified as *aged sea salt* (3%), *OC* (2%), *V*
(0.7%) and *Cu-Pb* (0.4%). If the queried oxalate particle numbers were considered representative of
the whole ATOFMS dataset, then biomass burning emissions play a large role in the fate of particle
phase oxalate in the western Mediterranean.

525 The ATOFMS querying approach indicated a prevalence of oxalate mixed with K-rich particles,
however correlations between PILS-IC oxalate and K-rich mass were poor; better correlations were
found with EC-rich and K-rich mass concentrations combined (R^2=0.55), suggesting either that more
EC particles actually contained oxalate than was detected or another particle type transported in the
same air mass but which was not detected by the ATOFMS. Moderate correlations were also found

530 between oxalate and LV-OOA (R^2=0.54), WSOC (R^2=0.55) and BC (R^2=0.55) mass concentrations
(for the period 21st June-4th August); hourly mass concentrations for these species are shown in
Figure 11 (mean concentration of oxalate: 9.8 ng/m^3). Oxalic acid is often the single most abundant
water-soluble organic compound identified in ambient aerosols (Yu et al., 2005), which explains the
agreement between oxalate and WSOC mass concentrations. While the humidity was relatively high

535 (average of 70%) throughout the two campaigns, so too was the solar radiation, with few instances
of cloud or fog formation at the site. The association with SV-OOA also supports photochemical
oxidation as the dominant oxalate formation mechanism.

3.5.2 MSA

MSA is a well-established tracer for marine phytoplankton activity (Hallquist et al., 2009; Gaston
540 et al., 2010), formed from heterogeneous OH (daytime) and homogeneous NO$_3$ (nighttime) oxida-
tion of DMS, the enzymatic cleavage product of dimethylsulfoniopropionate (DMSP), a compound
produced by oceanic phytoplankton. It is therefore a good indicator of biogenic (marine) sulfate and
its presence in aerosols typically indicates that they have undergone some marine transport, rather
than being produced locally (Gaston et al., 2010). While MSA has been proposed to primarily con-
545 tribute to particle growth in the atmosphere (Kreidenweis et al., 1989; Wyslouzil et al., 1991a, b),

Atmospheric
Chemistry
and Physics
Discussions

there is evidence that MSA can also contribute to new particle formation (Dawson et al., 2012; Willis et al., 2016). Recently, Sellegri et al. (2016) showed that iodine-containing species are likely precursors to new particle formation in the Mediterranean; a query of the ATOFMS ADRIMED and SAF-MED dataset for iodine (m/z -127) only returned 34 particles containing this ion. Iodine is

550   rarely reported in ATOFMS studies and even then it is usually in low numbers of particles; Beddows et al. (2004) found ~3600 $PM_{2.5}$ ATOFMS particles containing iodine at a rural background site in the UK. Both MSA and sulfate influence particle hygroscopicity, meaning that the enhanced production of either of these species by anthropogenic particle types could have implications for subsequent cloud droplet formation in both marine and inland environments (Lee et al., 2010; O'Dowd et al.,

555   2004).

MSA was identified in 2700 particles (0.2% of total particles ionised). Sulfate was also found in all of these. The mixing states derived from the querying approach largely agrees with those from the general approach. Similar to oxalate, enhanced partitioning of MSA was observed for biomass combustion particles. Particles similar to the *K-SO$_X$*, *EC-K-SO$_X$* and *K-EC-SO$_X$* classes accounted

560   for 45%, 25% and 11% of the MSA queried particles. *EC-V, V* and *Cu-Pb* classes contributed 11%, 4% and 1% respectively.

The preference for partitioning to combustion particles is in contrast to findings from Riverside, California (Gaston et al., 2010) where only small fractions of carbonaceous ATOFMS particle types contained MSA, and Cork, Ireland (Healy et al., 2010), where only one ATOFMS particle class

565   of several carbonaceous classes identified was internally mixed with MSA. It has been suggested that accumulation of secondary species during transport over urban regions can potentially mask the detection of MSA by ATOFMS in carbonaceous particles (Pratt and Prather, 2009).

In addition, it has been demonstrated that the oxidation of biogenically emitted DMS to form MSA, can be catalysed by vanadium, which has also been shown to enhance the conversion of

570   anthropogenically produced SO_2 to sulfate (Ault et al., 2010). About 40% of OC-V-sulfate (residual fuel combustion primarily from ships) particles and 33% of aged sea salt particles in Riverside contained MSA. No MSA could be clearly identified in aged sea salt particles in Corsica; m/z -95 was only found in fresh sea salt particles and was likely a result of $NaCl_2$ as it was present in the typical isotopic ratio i.e. its signal was smaller than m/z -93. This is again in contrast to the study

575   in Cork harbour (Healy et al., 2010), where none of the V-rich shipping classes were associated with MSA. However, the authors note that the sampling site in Cork Harbour was very close to shipping berths, so most shipping particles detected were expected to be freshly emitted. *K-OC-SO$_X$* particles, identified with the general clustering approach, produced average mass spectra with MSA signals. This was not supported by the querying approach; no OC-rich particles were found to

580   contain MSA, or at least so few as to not resolve into their own clusters. No Amine particles were identified in the MSA query. As discussed earlier, the presence of MSA in TMA and other amine-containing particles is possible, as indicated by laboratory studies of particle formation and growth

Atmospheric
Chemistry
and Physics
Discussions

from reactions between MSA, TMA (or methylamine and DMA) and water (Chen et al., 2015a, b). Amines have been frequently observed in marine aerosol (Facchini et al., 2008; Gaston et al., 2010; Müller et al., 2009; Sorooshian et al., 2009), and particulate amine levels have been found to correlate with particulate MSA levels (Sorooshian et al., 2009). Facchini et al. (2008) observed that MSA, DMA, and diethylamine were the most abundant organic species detected in fine particles in the North Atlantic during periods of high biological activity.

585

The remaining 3% of MSA queried particles was accounted for by particles containing dust tracers (Fe, Ca, Al). The Riverside study found that no MSA was found on submicron dust and only 3% of supermicron dust contained MSA (Gaston et al., 2010). The authors expected this since the dust they observed was locally produced, unlike MSA. In contrast, internally mixed OC, sea salt, sulfate, titanium (dust) and MSA formed particles $1 - 2$ μm in size at Mace Head during the EUCAARI project Dall'Osto et al. (2010) and were associated with a period of subtropical maritime air originating from the Azores high-pressure region. The number of dust particles identified with the MSA query in this work were statistically too few to consider submicron/supermicron ratios; from these previous studies it is not unusual to detect MSA on dust particles, however it is unlikely that they represent significant surfaces for MSA to condense onto as most of the MSA mass measured in the Mediterranean to date has been found in the submicron fraction. This observation is also echoed by Gaston et al. (2010); 67% of the submicron particles in Riverside contained MSA.

590

595

600

In Riverside MSA-containing particles were also associated with fog processing markers $^{81}HSO_3^-$ and hydroxymethanesulfonate (HMS, $^{111}HOCH_2SO_3^-$), highlighting aqueous phase chemistry as an important pathway in MSA formation (Bardouki and Rosa, 2002), as well as the hygroscopic nature of MSA (Barnes et al., 2006). Other studies correlated HMS with relative humidity (RH) during stagnant fog events (Whiteaker and Prather, 2003), however in Riverside the HMS correlation with MSA suggested HMS formation was not due to local increases in RH; rather MSA-particles had undergone aqueous phase processing either in the marine environment or during subsequent transport. Unfortunately queries for m/z -81 and -111 did not return a statistically useful number of particles, and the summed signal for both of these groups was too low to produce a statistically useful time series.

605

610

Hourly PILS-IC mass concentrations of MSA (average of 21 ng/m^3; lower than those measured in Paris; average of 122 ng/m^3; Crippa et al. (2013) compared to Mace Head, Ireland and Erdemli, Turkey) shown in Figure 12, did not correlate with any ATOFMS particle numbers or mass concentrations, or with any other measurements over the whole sampling period. However, some correlations were found for certain periods; from 7-15th July MSA mass agreed well with that of PILS-IC NO$_3^-$, while from 23rd July – 3rd August moderate correlations were found with PILS-IC NO$_3^-$ (R^2=0.53), SO$_4^{2-}$ (R^2=0.48) and NH$_4^+$ (R^2=0.54), and ACSM NO$_3^-$ (R^2=0.46). Increases in MSA mass coincided with sea salt events during Period 2 (Figure 12), although there were no good corre-

615

Atmospheric
Chemistry
and Physics
Discussions

lations with SSA concentration, suggesting MSA was not present on sea salt particles but formation

620 was enhanced by the influx of marine air masses.

4 Conclusions

As part of ChArMEx, two special observation periods on Corsica Island aimed to understand how the physical, chemical, optical properties and vertical distribution of aerosols affect the Mediterranean climate (ADRIMED), as well as develop a better understanding of the origins and particle proper-

625 ties of secondary organic aerosols (SAF-MED). Chemical composition is critical to achieving these aims. A single particle mass spectrometer (ATOFMS) provided detailed information on the mixing states and thereby sources of background aerosol in the western Mediterranean. Airmass trajectories and concurrent observations at the site were used to interpret ATOFMS observations. Overall, 27 distinct ATOFMS particle classes were identified from 1.2 million single particle mass spectra

630 and grouped into 8 general categories: EC, K-rich, Na-rich, Amines, OC-rich, V-rich, Fe-rich and Ca-rich. Mass concentrations were reconstructed for the ATOFMS particle classes and were in good agreement with other quantitative measurements (PM_1, ACSM species, BC). Total ATOFMS estimated mass ($PM_{2.5}$) accounted for 70-90% of PM_{10} mass, most of which was comprised of regionally transported aerosols containing fossil fuel combustion (EC-rich) particles, and K-rich particles

635 from biomass burning in northern Italy and the region surrounding the Black Sea, the accumulation of which was favoured by repeated and extended periods of air mass stagnation over the western Mediterranean. Amine-containing particles were also assigned to regionally transported combustion sources, both fossil fuel and biomass burning. Previous studies of aminecontaining particles found a strong dependence on relative humidity; this was not the case during these two campaigns,

640 suggesting these particles were not formed locally. Three other sources were also identified by the ATOFMS: local biomass burning, marine and shipping. Local biomass burning particles contributed little to $PM_{2.5}$ particle numbers and mass concentrations but were easily distinguished from regional combustion particles; no local sources of fossil fuel combustion were identified. Although the local emissions did not contribute significantly to particle number or mass concentrations the observa-

645 tions serve to highlight the ability of single particle measurements to distinguish between local and regional aerosol sources. Marine emissions comprised fresh and aged sea salt, the former detected mostly during one 5-day event and the latter detected throughout the sampling period. Mineral dust was not efficiently detected by the ATOFMS. Shipping particles, identified using markers for heavy fuel oil combustion, were identified as aged regional emissions which made only a small contribu-

650 tion to $PM_{2.5}$ particle numbers and mass concentrations. A query of the mixing states of oxalate, a photochemically aged aerosol marker, and MSA, a biogenic marine emissions marker showed that the majority of particles containing oxalate also contained K and sulfate, indicative of aged biomass burning emissions. MSA was also strongly associated with biomass burning particles and to a lesser

Atmospheric
Chemistry
and Physics
Discussions

extent with Shipping particles – probably related to transport time in the marine boundary layer.

655 Quantitative measurements by TEOM demonstrated that PM_1 particles accounted for most of PM_{10} mass concentrations over the whole sampling period. ACSM (PM_1) and PILS-IC (PM_{10}) sulfate and ammonium mass concentrations were very similar, indicating most of the mass of these species was in the PM_1 fraction. Accordingly, organics (36%), sulfate (16%) and ammonium (10%) constituted most of the PM_{10} mass. Mass concentrations of EC and K-rich particles were in good agreement

660 with those of ACSM sulfate, ammonium and the LV-OOA factor (which accounted for 54% of the organics), and BC. ATOFMS mass spectra provided valuable source markers, allowing the identification of fossil fuel and biomass burning combustion sources. Combined, this information shows these sources provided the primary particles, containing EC and OC, which then accumulated ammonium, sulfate and alkylamines during regional transport. The Mediterranean is a crossroad for air

665 masses transporting different types of aerosols from natural and anthropogenic origins. Identifying these sources and apportioning aerosol mass to them is a key component of future work to mitigate their effects on the Mediterranean climate.

Author contributions. PILS-IC, ACSM, TEOM PM_{10}, TEOM PM_1 and MAAP data were provided by J. Sciare; SMPS, OPS and meteorological data were provided by Météo-France. J. Arndt prepared

670 the manuscript with contributions from all co-authors.

Atmospheric
Chemistry
and Physics
Discussions

Open Access

EGU

References

680

Allen, J., Fergenson, D., Gard, E., Hughes, L., Morrical, B., Kleeman, M., Gross, D., Gälli, M., Prather, K.,
and Cass, G.: Particle Detection Efficiencies of Aerosol Time of Flight Mass Spectrometers under Ambient
Sampling Conditions, Environmental Science & Technology, 34, 211–217, doi:10.1021/es9904179, http:
//pubs.acs.org/doi/abs/10.1021/es9904179, 2000.

685 a.R. Lea-Langton, Baeza-Romero, M., Boman, G., Brooks, B., Wilson, A., Atika, F., Bartle, K.,
Jones, J., and Williams, A.: A study of smoke formation from wood combustion, Fuel Processing
Technology, 137, 327–332, doi:10.1016/j.fuproc.2015.03.020, http://linkinghub.elsevier.com/retrieve/pii/
S0378382015001307, 2015.

Ault, A., Moore, M., Furutani, H., and Prather, K.: Impact of emissions from the Los Angeles Port region on
690 San Diego air quality during regional transport events, Environmental Science & Technology, 43, 3500–
3506, doi:10.1021/es8018918, http://pubs.acs.org/doi/abs/10.1021/es8018918http://www.ncbi.nlm.nih.gov/
pubmed/19544846, 2009.

Ault, A., Gaston, C., Wang, Y., Dominguez, G., Thiemens, M., and Prather, K.: Characterization of the Single
Particle Mixing State of Individual Ship Plume Events Measured at the Port of Los Angeles., Environmen-
695 tal Science & Technology, 44, 1954–1061, doi:10.1021/es902985h, http://www.ncbi.nlm.nih.gov/pubmed/
20148582, 2010.

Barnes, I., Hjorth, J., and Mihalopoulos, N.: Dimethyl sulfide and dimethyl sulfoxide and their oxidation in
the atmosphere., Chemical Reviews, 106, 940–75, doi:10.1021/cr020529+, http://www.ncbi.nlm.nih.gov/
pubmed/16522014, 2006.

700 Bates, T. S., Quinn, P. K., Frossard, A. A., Russell, L. M., Hakala, J., Petäjä, T., Kulmala, M., Covert, D. S.,
Cappa, C. D., Li, S.-M., Hayden, K. L., Nuaaman, I., McLaren, R., Massoli, P., Canagaratna, M. R., Onasch,
T. B., Sueper, D., Worsnop, D. R., and Keene, W. C.: Measurements of ocean derived aerosol off the coast
of California, Journal of Geophysical Research: Atmospheres, 117, n/a–n/a, doi:10.1029/2012JD017588,
http://doi.wiley.com/10.1029/2012JD017588, 2012.

705 Becagli, S., Anello, F., Bommarito, C., Cassola, F., Calzolai, G., Di Iorio, T., di Sarra, A., Gómez-Amo,
J.-L., Lucarelli, F., Marconi, M., Meloni, D., Monteleone, F., Nava, S., Pace, G., Severi, M., Sfer-
lazzo, D. M., Traversi, R., and Udisti, R.: Constraining the ship contribution to the aerosol of the Cen-
tral Mediterranean, Atmospheric Chemistry and Physics Discussions, 0, 1–32, doi:10.5194/acp-2016-489,
http://www.atmos-chem-phys-discuss.net/acp-2016-489/, 2016.

710 Beddows, D. C. S., Donovan, R. J., Harrison, R. M., Heal, M. R., Kinnersley, R. P., King, M. D., Nicholson,
D. H., and Thompson, K. C.: Correlations in the chemical composition of rural background atmospheric
aerosol in the UK determined in real time using time-of-flight mass spectrometry, Journal of Environmental
Monitoring, 6, 124, doi:10.1039/b311209h, http://xlink.rsc.org/?DOI=b311209h, 2004.

Beekmann, M., Prévôt, A. S. H., Drewnick, F., Sciare, J., Pandis, S. N., Denier Van Der Gon, H. A. C., Crippa,
715 M., Freutel, F., Poulain, L., Ghersi, V., Rodriguez, E., Beirle, S., Zotter, P., Von Der Weiden-Reinmüller,
S. L., Bressi, M., Fountoukis, C., Petetin, H., Szidat, S., Schneider, J., Rosso, A., El Haddad, I., Megaritis,
A., Zhang, Q. J., Michoud, V., Slowik, J. G., Moukhtar, S., Kolmonen, P., Stohl, A., Eckhardt, S., Borbon,
A., Gros, V., Marchand, N., Jaffrezo, J. L., Schwarzenboeck, A., Colomb, A., Wiedensohler, A., Borrmann,
S., Lawrence, M., Baklanov, A., and Baltensperger, U.: In situ, satellite measurement and model evidence

Atmospheric
Chemistry
and Physics
Discussions

720 on the dominant regional contribution to fine particulate matter levels in the Paris megacity, Atmospheric
     Chemistry and Physics, 15, 9577–9591, doi:10.5194/acp-15-9577-2015, 2015.

     Bein, K., Zhao, Y., Pekney, N., Davidson, C., Johnston, M., and Wexler, A.: Identification of sources
     of atmospheric PM at the Pittsburgh Supersite—Part II: Quantitative comparisons of single par-
     ticle, particle number, and particle mass measurements, Atmospheric Environment, 40, 424–444,
725 doi:10.1016/j.atmosenv.2006.01.064, http://linkinghub.elsevier.com/retrieve/pii/S1352231006005966, 2006.

     Bergametti, G., Dutot, A.-L., Buat-Ménard, P., Losno, R., and Remoudaki, E.: Seasonal variability of the el-
     emental composition of atmospheric aerosol particles over the northwestern Mediterranean, Tellus, 41B,
     353–361, doi:10.1111/j.1600-0889.1989.tb00314.x, 1989.

     Bhave, P., Fergenson, D., Prather, K., and Cass, G.: Source apportionment of fine particulate matter by clustering
730 single-particle data: tests of receptor model accuracy., Environmental Science & Technology, 35, 2060–72,
     http://www.ncbi.nlm.nih.gov/pubmed/11393988, 2001.

     Bhave, P., Kleeman, M., Allen, J., Hughes, L., Prather, K., and Cass, G.: Evaluation of an Air Quality Model
     for the Size and Composition of Source-Oriented Particle Classes, Environmental Science & Technology,
     36, 2154–2163, doi:10.1021/es0112700, http://pubs.acs.org/doi/abs/10.1021/es0112700, 2002.

735 Cahill, J., Suski, K., Seinfeld, J., Zaveri, R., and Prather, K.: The mixing state of carbonaceous aerosol particles
     in northern and southern California measured during CARES and CalNex 2010, Atmospheric Chemistry and
     Physics, 12, 10 989–11 002, doi:10.5194/acp-12-10989-2012, http://www.atmos-chem-phys.net/12/10989/
     2012/, 2012.

     Cahill, J. F., Darlington, T. K., Wang, X., Mayer, J., Spencer, M. T., Holecek, J. C., Reed, B. E.,
740 and Prather, K. A.: Development of a High-Pressure Aerodynamic Lens for Focusing Large Parti-
     cles (4–10 μm) into the Aerosol Time-of-Flight Mass Spectrometer, Aerosol Science and Technology,
     48, 948–956, doi:10.1080/02786826.2014.947400, http://www.tandfonline.com/doi/abs/10.1080/02786826.
     2014.947400{#}.VOXEiPmsUgo, 2014.

     Chan, L. P. and Chan, C. K.: Role of the aerosol phase state in ammonia/amines exchange reactions., Environ-
745 mental science & technology, 47, 5755–62, doi:10.1021/es4004685, http://www.ncbi.nlm.nih.gov/pubmed/
     23668831, 2013.

     Chen, H., Ezell, M. J., Arquero, K. D., Varner, M. E., Dawson, M. L., Gerber, R. B., and Finlayson-
     Pitts, B. J.: New particle formation and growth from methanesulfonic acid, trimethylamine and wa-
     ter, Phys. Chem. Chem. Phys., 17, 13 699–13 709, doi:10.1039/C5CP00838G, http://xlink.rsc.org/?DOI=
750 C5CP00838G, 2015a.

     Chen, H., Varner, M. E., Gerber, R. B., and Finlayson-Pitts, B. J.: Reactions of Methanesulfonic Acid
     with Amines and Ammonia as a Source of New Particles in Air, The Journal of Physical Chemistry B,
     p. 151005113722003, doi:10.1021/acs.jpcb.5b07433, http://pubsdc3.acs.org/doi/abs/10.1021/acs.jpcb.5b07433,
     2015b.

755 Corbin, J., Rehbein, P., Evans, G., and Abbatt, J.: Combustion particles as ice nuclei in an urban en-
     vironment: Evidence from single-particle mass spectrometry, Atmospheric Environment, 51, 286–292,
     doi:10.1016/j.atmosenv.2012.01.007, http://linkinghub.elsevier.com/retrieve/pii/S1352231012000106, 2012.

     Crippa, M., El Haddad, I., Slowik, J. G., DeCarlo, P. F., Mohr, C., Heringa, M. F., Chirico, R., Marchand, N.,
     Sciare, J., Baltensperger, U., and Prévôt, A. S. H.: Identification of marine and continental aerosol sources in

Atmospheric
Chemistry
and Physics
Discussions

760   Paris using high resolution aerosol mass spectrometry, Journal of Geophysical Research: Atmospheres, 118, 1950–1963, doi:10.1002/jgrd.50151, http://doi.wiley.com/10.1002/jgrd.50151, 2013.

Dall'Osto, M. and Harrison, R.: Chemical characterisation of single airborne particles in Athens (Greece) by ATOFMS, Atmospheric Environment, 40, 7614–7631, doi:10.1016/j.atmosenv.2006.06.053, http://linkinghub.elsevier.com/retrieve/pii/S1352231006007242, 2006.

765   Dall'Osto, M., Beddows, D., Kinnersley, R., Harrison, R., Donovan, R., and Heal, M.: Characterization of individual airborne particles by using aerosol time-of-flight mass spectrometry at Mace Head, Ireland, Journal of Geophysical Research, 109, doi:10.1029/2004JD004747, http://www.agu.org/pubs/crossref/2004/2004JD004747.shtml, 2004.

Dall'Osto, M., Booth, M., Smith, W., Fisher, R., and Harrison, R.: A Study of the Size Distributions and the
770   Chemical Characterization of Airborne Particles in the Vicinity of a Large Integrated Steelworks, Aerosol Science and Technology, 42, 981–991, doi:10.1080/02786820802339587, 2008.

Dall'Osto, M., Harrison, R., Highwood, E., O'Dowd, C., Ceburnis, D., Querol, X., and Achterberg, E.: Variation of the mixing state of Saharan dust particles with atmospheric transport, Atmospheric Environment, 44, 3135–3146, doi:10.1016/j.atmosenv.2010.05.030, http://linkinghub.elsevier.com/retrieve/pii/
775   S1352231010004036, 2010.

Dall'Osto, M., Querol, X., Alastuey, A., Minguillon, M. C., Alier, M., Amato, F., Brines, M., Cusack, M., Grimalt, J. O., Karanasiou, A., Moreno, T., Pandolfi, M., Pey, J., Reche, C., Ripoll, A., Tauler, R., Van Drooge, B. L., Viana, M., Harrison, R. M., Gietl, J., Beddows, D., Bloss, W., O'Dowd, C., Ceburnis, D., Martucci, G., Ng, N. L., Worsnop, D., Wenger, J., Mc Gillicuddy, E., Sodeau, J., Healy, R., Lucarelli, F.,
780   Nava, S., Jimenez, J. L., Gomez Moreno, F., Artinano, B., Prévôt, A. S. H., Pfaffenberger, L., Frey, S., Wilsenack, F., Casabona, D., Jiménez-Guerrero, P., Gross, D., and Cots, N.: Presenting SAPUSS: Solving Aerosol Problem by Using Synergistic Strategies in Barcelona, Spain, Atmospheric Chemistry and Physics, 13, 8991–9019, doi:10.5194/acp-13-8991-2013, http://www.atmos-chem-phys.net/13/8991/2013/, 2013.

Dall'Osto, M., Beddows, D. C. S., Gietl, J. K., Olatunbosun, O. a., Yang, X., and Harrison, R. M.: Charac-
785   teristics of tyre dust in polluted air: Studies by single particle mass spectrometry (ATOFMS), Atmospheric Environment, 94, 224–230, doi:10.1016/j.atmosenv.2014.05.026, http://adsabs.harvard.edu/abs/2014AtmEn..94..224D$\delimiter"026E30F$nhttp://www.sciencedirect.com/science/article/pii/S1352231014003732$\delimiter"026E30F$nhttp://www.sciencedirect.com/science/article/pii/S1352231014003732/pdfft?md5=30710d14690714c664fffd21dd39ae8c{&}pid=1-s2.0-S13522310140037, 2014.

790   Dall'Osto, M., Beddows, D. C. S., McGillicuddy, E. J., Esser-Gietl, J. K., Harrison, R. M., and Wenger, J. C.: On the simultaneous deployment of two single particle mass spectrometers at an urban background and a road side site during SAPUSS, Atmospheric Chemistry and Physics Discussions, pp. 1–50, doi:10.5194/acp-2015-986, http://www.atmos-chem-phys-discuss.net/acp-2015-986/, 2016.

Dawson, M. L., Varner, M. E., Perraud, V., Ezell, M. J., Gerber, R. B., and Finlayson-Pitts, B. J.: Simplified
795   mechanism for new particle formation from methanesulfonic acid, amines, and water via experiments and ab initio calculations., Proceedings of the National Academy of Sciences of the United States of America, 109, 18 719–24, doi:10.1073/pnas.1211878109, http://www.pubmedcentral.nih.gov/articlerender.fcgi?artid=3503172{&}tool=pmcentrez{&}rendertype=abstract, 2012.

Atmospheric
Chemistry
and Physics
Discussions

de la Paz, D., Vedrenne, M., Borge, R., Lumbreras, J., de Andrés, J., Pérez, J., Rodríguez, E., Karana-
800   siou, A., Moreno, T., Boldo, E., and Linares, C.: Modelling Saharan dust transport into the Mediter-
ranean basin with CMAQ, Atmospheric Environment, 70, 337–350, doi:10.1016/j.atmosenv.2013.01.013,
http://linkinghub.elsevier.com/retrieve/pii/S1352231013000265, 2013.

DeCarlo, P., Slowik, J., Worsnop, D., Davidovits, P., and Jimenez, J.: Particle Morphology and Den-
sity Characterization by Combined Mobility and Aerodynamic Diameter Measurements. Part
805   1: Theory, Aerosol Science and Technology, 38, 1185–1205, doi:10.1080/027868290903907,
http://www.informaworld.com/openurl?genre=article{&}doi=10.1080/027868290903907{&}magic=
crossref‖D404A21C5BB053405B1A640AFFD44AE3, 2004.

Denjean, C., Cassola, F., Mazzino, A., Triquet, S., Chevaillier, S., Grand, N., Bourrianne, T., Mom-
boisse, G., Sellegri, K., Schwarzenbock, A., Freney, E., Mallet, M., and Formenti, P.: Size distribu-
810   tion and optical properties of mineral dust aerosols transported in the western Mediterranean, Atmos.
Chem. Phys., 16, 1081–1104, doi:10.5194/acp-16-1081-2016, http://www.atmos-chem-phys.net/16/1081/
2016/http://www.atmos-chem-phys.net/16/1081/2016/acp-16-1081-2016.pdf, 2016.

Denkenberger, K. A., Moffet, R. C., Holecek, J. C., Rebotier, T. P., and Prather, K. A.: Real-Time, Single-
Particle Measurements of Oligomers in Aged Ambient Aerosol Particles, Environmental Science & Tech-
815   nology, 41, 5439–5446, doi:10.1021/es070329l, http://pubs.acs.org/doi/abs/10.1021/es070329l, 2007.

Draxler, R. R. and Hess, G.: An Overview of the HYSPLIT_4 Modelling System for Trajectories, Dispersion,
and Deposition, Australian Meteorological Magazine, 47, 295–308, 1998.

El Haddad, I., Marchand, N., Wortham, H., Piot, C., Besombes, J. L., Cozic, J., Chauvel, C., Armengaud, A.,
Robin, D., and Jaffrezo, J. L.: Primary sources of PM2.5organic aerosol in an industrial Mediterranean city,
820   Marseille, Atmospheric Chemistry and Physics, 11, 2039–2058, doi:10.5194/acp-11-2039-2011, 2011.

El Haddad, I., D'Anna, B., Temime-Roussel, B., Nicolas, M., Boreave, A., Favez, O., Voisin, D., Sciare, J.,
George, C., Jaffrezo, J. L., Wortham, H., and Marchand, N.: Towards a better understanding of the origins,
chemical composition and aging of oxygenated organic aerosols: Case study of a Mediterranean industri-
alized environment, Marseille, Atmospheric Chemistry and Physics, 13, 7875–7894, doi:10.5194/acp-13-
825   7875-2013, 2013.

Facchini, M., Decesari, S., Rinaldi, M., Carbone, C., Finessi, E., Mircea, M., Fuzzi, S., Moretti, F., Tagliavini,
E., Ceburnis, D., and O'Dowd, C.: Important source of marine secondary organic aerosol from biogenic
amines., Environmental Science & Technology, 42, 9116–9121, doi:10.1021/es8018385, http://www.ncbi.
nlm.nih.gov/pubmed/19174880, 2008.

830   Favez, O., Cachier, H., Sciare, J., and Le Moullec, Y.: Characterization and contribution to
PM2.5 of semi-volatile aerosols in Paris (France), Atmospheric Environment, 41, 7969–7976,
doi:10.1016/j.atmosenv.2007.09.031, 2007.

Ferge, T., Karg, E., Schröppel, a., Coffee, K. R., Tobias, H. J., Frank, M., Gard, E. E., and Zimmermann, R.:
Fast determination of the relative elemental and organic carbon content of aerosol samples by on-line single-
835   particle aerosol time-of-flight mass spectrometry, Environmental Science and Technology, 40, 3327–3335,
doi:10.1021/es050799k, 2006.

Fitzgerald, E., Ault, A. P., Zauscher, M. D., Mayol-Bracero, O. L., and Prather, K. A.: Comparison of the mixing state of long-range transported Asian and African mineral dust, Atmospheric Environment, 115, 19–25, doi:10.1016/j.atmosenv.2015.04.031, http://linkinghub.elsevier.com/retrieve/pii/S1352231015300340, 2015.

840 Furutani, H., Dall'Osto, M., Roberts, G., and Prather, K.: Assessment of the relative importance of atmospheric aging on CCN activity derived from field observations, Atmospheric Environment, 42, 3130–3142, doi:10.1016/j.atmosenv.2007.09.024, http://linkinghub.elsevier.com/retrieve/pii/S1352231007008084, 2008.

Gangoiti, G.: Long-range transport and re-circulation of pollutants in the western Mediterranean during the project Regional Cycles of Air Pollution in the West-Central Mediterranean Area, Atmospheric Environ-
845 ment, 35, 6267–6276, doi:10.1016/S1352-2310(01)00440-X, http://www.sciencedirect.com/science/article/pii/S135223100100440Xhttp://linkinghub.elsevier.com/retrieve/pii/S135223100100440X, 2001.

Gard, E., Mayer, J. E., Morrical, B. D., Dienes, T., Fergenson, D. P., and Prather, K. A.: Real-Time Analysis of Individual Atmospheric Aerosol Particles: Design and Performance of a Portable ATOFMS, Analytical Chemistry, 69, 4083–4091, doi:10.1021/ac970540n, http://pubs.acs.org/doi/abs/10.1021/ac970540n, 1997.

850 Gard, E. E., Kleeman, M. J., Gross, D. S., Hughes, L. S., Allen, J. O., Morrical, B. D., Fergenson, D. P., Dienes, T., Galli, M. E., Johnson, R. J., Cass, G. R., and Prather, K. A.: Direct Observation of Heterogeneous Chemistry in the Atmosphere, Science, 279, 1184–1187, doi:10.1126/science.279.5354.1184, http://www.sciencemag.org/cgi/doi/10.1126/science.279.5354.1184, 1998.

Gaston, C., Pratt, K., Qin, X., and Prather, K.: Real-Time detection and mixing state of methanesulfonate
855 in single particles at an inland urban location during a phytoplankton bloom., Environmental Science & Technology, 44, 1566–72, doi:10.1021/es902069d, http://www.ncbi.nlm.nih.gov/pubmed/20121235, 2010.

Giorio, C., Tapparo, A., Dall'Osto, M., Harrison, R. M., Beddows, D. C., Di Marco, C., and Nemitz, E.: Comparison of three techniques for analysis of data from an Aerosol Time-of-Flight Mass Spectrometer, Atmospheric Environment, 61, 316–326, doi:10.1016/j.atmosenv.2012.07.054, http://linkinghub.elsevier.com/
860 retrieve/pii/S1352231012007261, 2012.

Gross, D., Atlas, R., Rzeszotarski, J., Turetsky, E., Christensen, J., Benzaid, S., Olson, J., Smith, T., Steinberg, L., and Sulman, J.: Environmental chemistry through intelligent atmospheric data analysis, Environmental Modelling & Software, 25, 760–769, doi:10.1016/j.envsoft.2009.12.001, http://linkinghub.elsevier.com/retrieve/pii/S1364815209003041, 2010.

865 Gross, D. S., Gälli, M. E., Silva, P. J., and Prather, K. A.: Relative sensitivity factors for alkali metal and ammonium cations in single-particle aerosol time-of-flight mass spectra, Analytical Chemistry, 72, 416–422, doi:10.1021/ac990434g, http://www.ncbi.nlm.nih.gov/pubmed/10658339, 2000a.

Gross, D. S., Galli, M. E., Silva, P. J., Wood, S. H., Liu, D.-Y., and Prather, K. A.: Single Particle Characterization of Automobile and Diesel Truck Emissions in the Caldecott Tunnel, Aerosol Science and Technology,
870 32, 152–163, doi:10.1080/027868200303858, http://www.informaworld.com/openurl?genre=article&doi=10.1080/027868200303858&magic=crossref‖D404A21C5BB053405B1A640AFFD44AE3http://www.tandfonline.com/doi/abs/10.1080/027868200303858, 2000b.

Guazzotti, S., Whiteaker, J., Suess, D., Coffee, K., and Prather, K.: Real-time measurements of the chemical composition of size-resolved particles during a Santa Ana wind episode, California USA, Atmospheric
875 Environment, 35, 3229–3240, doi:10.1016/S1352-2310(01)00140-6, http://linkinghub.elsevier.com/retrieve/pii/S1352231001001406, 2001.

Guieu, C., Dulac, F., Desboeufs, K., Wagener, T., Pulido-Villena, E., Grisoni, J. M., Louis, F., Ridame, C., Blain, S., Brunet, C., Bon Nguyen, E., Tran, S., Labiadh, M., and Dominici, J. M.: Large clean mesocosms and simulated dust deposition: A new methodology to investigate responses of marine oligotrophic ecosystems to atmospheric inputs, Biogeosciences, 7, 2765–2784, doi:10.5194/bg-7-2765-2010, 2010.

Hallquist, M., Wenger, J. C., Baltensperger, U., Rudich, Y., Simpson, D., Claeys, M., Dommen, J., Donahue, N. M., George, C., Goldstein, a. H., Hamilton, J. F., Herrmann, H., Hoffmann, T., Iinuma, Y., Jang, M., Jenkin, M. E., Jimenez, J. L., Kiendler-Scharr, a., Maenhaut, W., McFiggans, G., Mentel, T. F., Monod, a., Prévôt, a. S. H., Seinfeld, J. H., Surratt, J. D., Szmigielski, R., and Wildt, J.: The formation, properties and impact of secondary organic aerosol: current and emerging issues, Atmos. Chem. Phys., 9, 5155–5236, doi:10.5194/acp-9-5155-2009, http://www.atmos-chem-phys.net/9/5155/2009/ $\delimiter"026E30F$nhttp://www.atmos-chem-phys.net/9/5155/2009/acp-9-5155-2009.pdf, 2009.

Harrison, R. M., Dall'Osto, M., Beddows, D. C. S., Thorpe, a. J., Bloss, W. J., Allan, J. D., Coe, H., Dorsey, J. R., Gallagher, M., Martin, C., Whitehead, J., Williams, P. I., Jones, R. L., Langridge, J. M., Benton, a. K., Ball, S. M., Langford, B., Hewitt, C. N., Davison, B., Martin, D., Petersson, K. F., Henshaw, S. J., White, I. R., Shallcross, D. E., Barlow, J. F., Dunbar, T., Davies, F., Nemitz, E., Phillips, G. J., Helfter, C., Di Marco, C. F., and Smith, S.: Atmospheric chemistry and physics in the atmosphere of a developed megacity (London): an overview of the REPARTEE experiment and its conclusions, Atmospheric Chemistry and Physics, 12, 3065–3114, doi:10.5194/acp-12-3065-2012, http://www.atmos-chem-phys.net/12/3065/2012/, 2012.

Healy, R., O'Connor, I, Hellebust, S., Allanic, A., Sodeau, J., and Wenger, J.: Characterisation of single particles from in-port ship emissions, Atmospheric Environment, 43, 6408–6414, doi:10.1016/j.atmosenv.2009.07.039, http://linkinghub.elsevier.com/retrieve/pii/S1352231009006529, 2009.

Healy, R. M., Hellebust, S., Kourtchev, I., Allanic, A., O'Connor, I. P., Bell, J. M., Healy, D. A., Sodeau, J. R., and Wenger, J. C.: Source apportionment of $PM_{2.5}$ in Cork Harbour, Ireland using a combination of single particle mass spectrometry and quantitative semi-continuous measurements, Atmospheric Chemistry and Physics, 10, 9593–9613, doi:10.5194/acp-10-9593-2010, http://www.atmos-chem-phys.net/10/9593/2010/, 2010.

Healy, R. M., Sciare, J., Poulain, L., Kamili, K., Merkel, M., Müller, T., Wiedensohler, A., Eckhardt, S., Stohl, A., Sarda-Estève, R., McGillicuddy, E., O'Connor, I. P., Sodeau, J. R., and Wenger, J. C.: Sources and mixing state of size-resolved elemental carbon particles in a European megacity: Paris, Atmospheric Chemistry and Physics, 12, 1681–1700, doi:10.5194/acp-12-1681-2012, http://www.atmos-chem-phys.net/12/1681/2012/, 2012.

Healy, R. M., Evans, G. J., Murphy, M., Sierau, B., Arndt, J., McGillicuddy, E., O'Connor, I. P., Sodeau, J. R., and Wenger, J. C.: Single-particle speciation of alkylamines in ambient aerosol at five European sites, Analytical and Bioanalytical Chemistry, 407, 5899–5909, doi:10.1007/s00216-014-8092-1, http://www.ncbi.nlm.nih.gov/pubmed/25146355http://link.springer.com/10.1007/s00216-014-8092-1, 2015.

Herich, H., Kammermann, L., Friedman, B., Gross, D., Weingartner, E., Lohmann, U., Spichtinger, P., Gysel, M., Baltensperger, U., and Cziczo, D.: Subarctic atmospheric aerosol composition: 2. Hygroscopic growth properties, Journal of Geophysical Research, 114, 1–14, doi:10.1029/2008JD011574, http://www.agu.org/pubs/crossref/2009/2008JD011574.shtml, 2009.

26

Atmospheric
Chemistry
and Physics
Discussions

Hu, D., Li, C., Chen, H., Chen, J., Ye, X., Li, L., Yang, X., Wang, X., Mellouki, A., and Hu, Z.: Hygroscopicity and optical properties of alkylaminium sulfates, Journal of Environmental Sciences, 26, 37–43, doi:10.1016/S1001-0742(13)60378-2, http://www.ncbi.nlm.nih.gov/pubmed/24649689http://linkinghub.elsevier.com/retrieve/pii/S1001074213603782, 2014.

920 Kanakidou, M., Mihalopoulos, N., Kindap, T., Im, U., Vrekoussis, M., Gerasopoulos, E., Dermitzaki, E., Unal, A., Koçak, M., Markakis, K., Melas, D., Kouvarakis, G., Youssef, A. F., Richter, A., Hatzianastassiou, N., Hilboll, A., Ebojie, F., Wittrock, F., von Savigny, C., Burrows, J. P., Ladstaetter-Weissenmayer, A., and Moubasher, H.: Megacities as hot spots of air pollution in the East Mediterranean, Atmospheric Environment, 45, 1223–1235, doi:10.1016/j.atmosenv.2010.11.048, http://linkinghub.elsevier.com/retrieve/pii/
925 S1352231010010162, 2011.

Karanasiou, A., Sitaras, I., Siskos, P., and Eleftheriadis, K.: Size distribution and sources of trace metals and n-alkanes in the Athens urban aerosol during summer, Atmospheric Environment, 41, 2368–2381, doi:10.1016/j.atmosenv.2006.11.006, 2007.

Karanasiou, A., Siskos, P., and Eleftheriadis, K.: Assessment of source apportionment by Positive Matrix Factorization analysis on fine and coarse urban aerosol size fractions, Atmospheric Environment, 43, 3385–3395,
930 doi:10.1016/j.atmosenv.2009.03.051, http://dx.doi.org/10.1016/j.atmosenv.2009.03.051, 2009.

Karanasiou, A., Moreno, T., Amato, F., Lumbreras, J., Narros, A., Borge, R., Tobías, A., Boldo, E., Linares, C., Pey, J., Reche, C., Alastuey, A., and Querol, X.: Road dust contribution to PM levels - Evaluation of the effectiveness of street washing activities by means of Positive Matrix Factorization, Atmospheric Environment, 45, 2193–2201, doi:10.1016/j.atmosenv.2011.01.067, http://dx.doi.org/10.1016/j.atmosenv.2011.
935 01.067, 2011.

Karanasiou, A., Querol, X., Alastuey, A., Perez, N., Pey, J., Perrino, C., Berti, G., Gandini, M., Poluzzi, V., Ferrari, S., de la Rosa, J., Pascal, M., Samoli, E., Kelessis, A., Sunyer, J., Alessandrini, E., Stafoggia, M., and Forastiere, F.: Particulate matter and gaseous pollutants in the Mediterranean
940 Basin: Results from the MED-PARTICLES project, Science of The Total Environment, 488-489, 297–315, doi:10.1016/j.scitotenv.2014.04.096, http://www.ncbi.nlm.nih.gov/pubmed/24836139http://linkinghub.elsevier.com/retrieve/pii/S0048969714006068, 2014.

Kreidenweis, S. M., Flagan, R. C., Seinfeld, J. H., and Okuyama, K.: Binary nucleation of methanesulfonic acid and water, Journal of Aerosol Science, 20, 585–607, doi:10.1016/0021-8502(89)90105-5, 1989.

945 Kubilay, N. and Saydam, A.: Trace elements in atmospheric particulates over the eastern Mediterranean; Concentrations, sources, and temporal variability, Atmospheric Environment, 29, 2289–2300, doi:10.1016/1352-2310(95)00101-4, 1995.

Lambert, D., Mallet, M., Ducrocq, V., Dulac, F., Gheusi, F., and Kalthoff, N.: CORSiCA: a Mediterranean atmospheric and oceanographic observatory in Corsica within the framework of HyMeX and ChArMEx,
950 Advances in Geosciences, 26, 125–131, doi:10.5194/adgeo-26-125-2011, 2011.

Lee, G., Park, J., Jang, Y., Lee, M., Kim, K.-R., Oh, J.-R., Kim, D., Yi, H.-I., and Kim, T.-Y.: Vertical variability of seawater DMS in the South Pacific Ocean and its implication for atmospheric and surface seawater DMS., Chemosphere, 78, 1063–70, doi:10.1016/j.chemosphere.2009.10.054, http://www.ncbi.nlm.nih.gov/pubmed/20079517, 2010.

Atmospheric
Chemistry
and Physics
Discussions

955 Lelieveld, J., Berresheim, H., Borrmann, S., Crutzen, P., Dentener, F., Fischer, H., Feichter, J., Flatau, P., Heland,
     J., Holzinger, R., Korrmann, R., Lawrence, M. G., Levin, Z., Markowicz, K. M., Mihalopoulos, N., Minikin,
     A., Ramanathan, V., De Reus, M., Roelofs, G. J., Scheeren, H. a., Sciare, J., Schlager, H., Schultz, M., Sieg-
     mund, P., Steil, B., Stephanou, E. G., Stier, P., Traub, M., Warneke, C., Williams, J., and Ziereis, H.: Global
     air pollution crossroads over the Mediterranean., Science, 298, 794–799, doi:10.1126/science.1075457,
960   http://www.ncbi.nlm.nih.gov/pubmed/12399583, 2002.

     Liu, D., Wenzel, R., Prather, K., Liu, D., Edgerton, E., and Prather, K.: Aerosol time-of-flight mass spec-
     trometry during the Atlanta Supersite Experiment: 1. Measurements, Journal of Geophysical Research,
     108, 8426, doi:10.1029/2001JD001562, http://www.agu.org/pubs/crossref/2003/2001JD001563.shtmlhttp:
     //www.agu.org/pubs/crossref/2003/2001JD001562.shtml, 2003.

965 Mallet, M., Dulac, F., Formenti, P., Nabat, P., Sciare, J., Roberts, G., Pelon, J., Ancellet, G., Tanré, D., Parol,
     F., di Sarra, A., Alados, L., Arndt, J., Auriol, F., Blarel, L., Bourrianne, T., Brogniez, G., Chazette, P.,
     Chevaillier, S., Claeys, M., D'Anna, B., Denjean, C., Derimian, Y., Desboeufs, K., Di Iorio, T., Doussin,
     J.-F., Durand, P., Féron, A., Freney, E., Gaimoz, C., Goloub, P., Gómez-Amo, J. L., Granados-Muñoz, M. J.,
     Grand, N., Hamonou, E., Jankowiak, I., Jeannot, M., Léon, J.-F., Maillé, M., Mailler, S., Meloni, D., Menut,
970 L., Momboisse, G., Nicolas, J., Podvin, J., Pont, V., Rea, G., Renard, J.-B., Roblou, L., Schepanski, K.,
     Schwarzenboeck, A., Sellegri, K., Sicard, M., Solmon, F., Somot, S., Torres, B., Totems, J., Triquet, S.,
     Verdier, N., Verwaerde, C., Wenger, J., Zapf, P., Brogniez, G., di Sarra, A., Alados-Arboledas, L., Arndt, J.,
     Auriol, F., Blarel, L., Bourrianne, T., Chazette, P., Chevaillier, S., Claeys, M., D'Anna, B., Derimian, Y.,
     Desboeufs, K., Di Iorio, T., Doussin, J.-F., Durand, P., Féron, A., Freney, E., Gaimoz, C., Goloub, P., Gómez-
975 Amo, J. L., Granados-Muñoz, M. J., Grand, N., Hamonou, E., Jankowiak, I., Jeannot, M., Léon, J.-F., Maillé,
     M., Mailler, S., Meloni, D., Menut, L., Momboisse, G., Nicolas, J., Podvin, T., Pont, V., Rea, G., Renard, J.-
     B., Roblou, L., Schepanski, K., Schwarzenboeck, A., Sellegri, K., Sicard, M., Solmon, F., Somot, S., Torres,
     B., Totems, J., Triquet, S., Verdier, N., Verwaerde, C., Waquet, F., Wenger, J., and Zapf, P.: Overview of the
     Chemistry-Aerosol Mediterranean Experiment/Aerosol Direct Radiative Forcing on the Mediterranean Cli-
980   mate (ChArMEx/ADRIMED) summer 2013 campaign, Atmos. Chem. Phys., 16, 455–504, doi:10.5194/acp-
     16-455-2016, http://www.atmos-chem-phys.net/16/455/2016/http://www.atmos-chem-phys.net/16/455/
     2016/acp-16-455-2016.pdfhttp://www.atmos-chem-phys-discuss.net/15/19615/2015/, 2016.

     Marmer, E. and Langmann, B.: Impact of ship emissions on the Mediterranean summertime
     pollution and climate: A regional model study, Atmospheric Environment, 39, 4659–4669,
985   doi:10.1016/j.atmosenv.2005.04.014, 2005.

     McGillicuddy, E. J.: Real Time Analysis of Atmospheric Single Particles in Urban Environments using Aerosol
     Time of Flight Mass Spectrometry, Doctoral, Univesity College Cork, 2014.

     Michoud, V., Sciare, J., Sauvage, S., Dusanter, S., Léonardis, T., Gros, V., Kalogridis, C., Zannoni, N., Feron,
     A., Petit, J.-E., Crenn, V., Baisnée, D., Sarda-Estève, R., Bonnaire, N., Marchand, N., DeWitt, L., Pey, J.,
990 Colomb, A., Gheusi, F., Szidat, S., Stavroulas, I., Borbon, A., and Locoge, N.: Organic carbon at a remote
     site of the western Mediterranean Basin: composition, sources and chemistry during the ChArMEx SOP2
     field experiment, Atmospheric Chemistry and Physics Discussions, 2016.

Atmospheric
Chemistry
and Physics
Discussions

Millán, M. and Salvador, R.: Photooxidant dynamics in the Mediterranean basin in summer: results from European research projects, Journal of Geophysical Research, 102, 8811–8823, doi:10.1029/96JD03610, http://onlinelibrary.wiley.com/doi/10.1029/96JD03610/full, 1997.

Millán, M., Mantilla, E., Salvador, R., Carratalá, A., Sanz, M., Alonso, L., Gangoiti, G., and Navazo, M.: Ozone cycles in the western Mediterranean basin: interpretation of monitoring data in complex coastal terrain, Journal of Applied Meteorology, 39, 487–508, doi:10.1175/1520-0450(2000)039<0487:OCITWM>2.0.CO;2, http://journals.ametsoc.org/doi/abs/10.1175/1520-0450(2000)039{%}3C0487:OCITWM{%}3E2.0.CO{%}3B2, 2000.

Millán, M. M., José Sanz, M., Salvador, R., and Mantilla, E.: Atmospheric dynamics and ozone cycles related to nitrogen deposition in the western Mediterranean, Environmental Pollution, 118, 167–186, doi:10.1016/S0269-7491(01)00311-6, http://www.ncbi.nlm.nih.gov/pubmed/11939281http://linkinghub.elsevier.com/retrieve/pii/S0269749101003116, 2002.

Moffet, R. and Prather, K.: In-situ measurements of the mixing state and optical properties of soot with implications for radiative forcing estimates., Proceedings of the National Academy of Sciences of the United States of America, 106, 11 872–7, doi:10.1073/pnas.0900040106, http://www.pubmedcentral.nih.gov/articlerender.fcgi?artid=2715487{&}tool=pmcentrez{&}rendertype=abstract, 2009.

Moffet, R., Desyaterik, Y., Hopkins, R., Tivanski, A., Gilles, M., Wang, Y., Shutthanandan, V., Molina, L., Abraham, R., Johnson, K., Mugica, V., Molina, M., Laskin, A., and Prather, K.: Characterization of Aerosols Containing Zn, Pb, and Cl from an Industrial Region of Mexico City, Environmental Science & Technology, 42, 7091–7097, doi:10.1021/es7030483, http://pubs.acs.org/doi/abs/10.1021/es7030483, 2008.

Moldanová, J., Fridell, E., Popovicheva, O., Demirdjian, B., Tishkova, V., Faccinetto, A., and Focsa, C.: Characterisation of particulate matter and gaseous emissions from a large ship diesel engine, Atmospheric Environment, 43, 2632–2641, doi:10.1016/j.atmosenv.2009.02.008, http://linkinghub.elsevier.com/retrieve/pii/S1352231009001253, 2009.

Monn, C., Braendli, O., Schaeppi, G., Schindler, C., Ackermann-Liebrich, U., and Leuenberger, P.: Particulate matter < 10 μm (PM10) and total suspended particulates (TSP) in urban, rural and alpine air in Switzerland, Atmospheric Environment, 29, 2565–2573, doi:10.1016/1352-2310(95)94999-U, http://www.sciencedirect.com/science/article/pii/135223109594999Uhttp://linkinghub.elsevier.com/retrieve/pii/135223109594999U, 1995.

Müller, C., Iinuma, Y., Karstensen, J., van Pinxteren, D., Lehmann, S., Gnauk, T., and Herrmann, H.: Seasonal variation of aliphatic amines in marine sub-micrometer particles at the Cape Verde islands, Atmospheric Chemistry and Physics Discussions, 9, 14 825–14 855, doi:10.5194/acpd-9-14825-2009, 2009.

Neubauer, K., Johnston, M., and Wexler, A.: On-line analysis of aqueous aerosols by laser desorption ionization, International Journal of Mass Spectrometry and Ion Processes, 163, 29–37, doi:10.1016/S0168-1176(96)04534-X, http://linkinghub.elsevier.com/retrieve/pii/S016811769604534X, 1997.

Neubauer, K., Johnston, M., and Wexler, A.: Humidity effects on the mass spectra of single aerosol particles, Atmospheric Environment, 32, 2521–2529, doi:10.1016/S1352-2310(98)00005-3, http://linkinghub.elsevier.com/retrieve/pii/S1352231098000053, 1998.

Atmospheric
Chemistry
and Physics
Discussions

Open Access

O'Dowd, C., Facchini, M., Cavalli, F., Ceburnis, D., Mircea, M., Decesari, S., Fuzzi, S., Yoon, Y., and Putaud, J.-P.: Biogenically driven organic contribution to marine aerosol., Nature, 431, 676–680, doi:10.1038/nature02959, 2004.

Pagels, J., Dutcher, D. D. D., Stolzenburg, M. M. R., Mcmurry, P. H. P., Gälli, M. E. M., and Gross, D. D. S.: Fine-particle emissions from solid biofuel combustion studied with single-particle mass spectrometry: Identification of markers for organics, soot, and ash components, Journal of Geophysical Research: Atmospheres, 118, 859–870, doi:10.1029/2012JD018389, http://doi.wiley.com/10.1029/2012JD018389, 2013.

Pey, J., Querol, X., and Alastuey, A.: Discriminating the regional and urban contributions in the North-Western Mediterranean: PM levels and composition, Atmospheric Environment, 44, 1587–1596, doi:10.1016/j.atmosenv.2010.02.005, http://linkinghub.elsevier.com/retrieve/pii/S1352231010001081, 2010.

Pratt, K., Hatch, L., and Prather, K.: Seasonal volatility dependence of ambient particle phase amines., Environmental Science & Technology, 43, 5276–81, http://www.ncbi.nlm.nih.gov/pubmed/19708353, 2009.

Pratt, K. A. and Prather, K. A.: Real-Time, Single-Particle Volatility, Size, and Chemical Composition Measurements of Aged Urban Aerosols, Environmental Science & Technology, 43, 8276–8282, doi:10.1021/es902002t, http://pubs.acs.org/doi/full/10.1021/es902002thttp://pubs.acs.org/doi/abs/10.1021/es902002t, 2009.

Pratt, K. A. and Prather, K. A.: Mass spectrometry of atmospheric aerosols-Recent developments and applications. Part II: On-line mass spectrometry techniques, Mass Spectrometry Reviews, 31, 17–48, doi:10.1002/mas.20330, http://doi.wiley.com/10.1002/mas.20330, 2012.

Pratt, K. a., Heymsfield, A. J., Twohy, C. H., Murphy, S. M., DeMott, P. J., Hudson, J. G., Subramanian, R., Wang, Z., Seinfeld, J. H., and Prather, K. A.: In Situ Chemical Characterization of Aged Biomass-Burning Aerosols Impacting Cold Wave Clouds, Journal of the Atmospheric Sciences, 67, 2451–2468, doi:10.1175/2010JAS3330.1, 2010.

Qin, X. and Prather, K.: Impact of biomass emissions on particle chemistry during the California Regional Particulate Air Quality Study, International Journal of Mass Spectrometry, 258, 142–150, doi:10.1016/j.ijms.2006.09.004, http://linkinghub.elsevier.com/retrieve/pii/S1387380606004222, 2006.

Qin, X., Bhave, P., and Prather, K.: Comparison of two methods for obtaining quantitative mass concentrations from aerosol time-of-flight mass spectrometry measurements., Analytical Chemistry, 78, 6169–78, doi:10.1021/ac060395q, http://www.ncbi.nlm.nih.gov/pubmed/16944899, 2006.

Qin, X., Pratt, K. a., Shields, L. G., Toner, S. M., and Prather, K. A.: Seasonal comparisons of single-particle chemical mixing state in Riverside, CA, Atmospheric Environment, 59, 587–596, doi:10.1016/j.atmosenv.2012.05.032, http://linkinghub.elsevier.com/retrieve/pii/S1352231012004815, 2012.

Querol, X., Alastuey, A., Puicercus, J., Mantilla, E., Miro, J., Lopez-Soler, A., Plana, F., and Artiñano, B.: Seasonal evolution of suspended particles around a large coal-fired power station: Particulate levels and sources, Atmospheric Environment, 32, 1963–1978, doi:10.1016/S1352-2310(97)00504-9, 1998a.

Querol, X., Alastuey, A., Puicercus, J., Mantilla, E., Ruiz, C., Lopez-Soler, A., Plana, F., and Juan, R.: Seasonal evolution of suspended particles around a large coal-fired power station: Chemical characterization, Atmospheric Environment, 32, 719–731, doi:10.1016/S1352-2310(97)00340-3, 1998b.

Querol, X., Alastuey, A., Rodríguez, S., Viana, M., Artíñano, B., Salvador, P., Mantilla, E., Do Santos, S. G., Patier, R. F., De La Rosa, J., De La Campa, a. S., Menéndez, M., and Gil, J. J.: Levels of particulate

Atmospheric
Chemistry
and Physics
Discussions

Open Access

matter in rural, urban and industrial sites in Spain, Science of the Total Environment, 334-335, 359–376, doi:10.1016/j.scitotenv.2004.04.036, 2004.

Querol, X., Alastuey, A., Pey, J., Cusack, M., Pérez, N., Mihalopoulos, N., Theodosi, C., Gerasopoulos, E., Kubilay, N., and Koçak, M.: Variability in regional background aerosols within the Mediterranean, Atmospheric Chemistry and Physics, 9, 4575–4591, doi:10.5194/acpd-9-10153-2009, 2009.

Rehbein, P. J. G., Jeong, C. H., McGuire, M. L., Yao, X., Corbin, J. C., and Evans, G. J.: Cloud and fog processing enhanced gas-to-particle partitioning of trimethylamine, Environmental Science and Technology, 45, 4346–4352, doi:10.1021/es1042113, 2011.

Reinard, M. and Johnston, M.: Ion formation mechanism in laser desorption ionization of individual nanoparticles., Journal of the American Society for Mass Spectrometry, 19, 389–99, doi:10.1016/j.jasms.2007.11.017, http://www.ncbi.nlm.nih.gov/pubmed/18191579, 2008.

Reinard, M., Adou, K., Martini, J., and Johnston, M.: Source characterization and identification by real-time single particle mass spectrometry, Atmospheric Environment, 41, 9397–9409, doi:10.1016/j.atmosenv.2007.09.001, http://linkinghub.elsevier.com/retrieve/pii/S1352231007007893, 2007.

Renard, J. B., Dulac, F., Berthet, G., Lurton, T., Vignelles, D., Jégou, F., Tonnelier, T., Jeannot, M., Couté, B., Akiki, R., Verdier, N., Mallet, M., Gensdarmes, F., Charpentier, P., Mesmin, S., Duverger, V., Dupont, J. C., Elias, T., Crenn, V., Sciare, J., Zieger, P., Salter, M., Roberts, T., Giacomoni, J., Gobbi, M., Hamonou, E., Olafsson, H., Dagsson-Waldhauserova, P., Camy-Peyret, C., Mazel, C., Décamps, T., Piringer, M., Surcin, J., and Daugeron, D.: LOAC: A small aerosol optical counter/sizer for ground-based and balloon measurements of the size distribution and nature of atmospheric particles-Part 2: First results from balloon and unmanned aerial vehicle flights, Atmospheric Measurement Techniques, 9, 3673–3686, doi:10.5194/amt-9-3673-2016, 2016.

Rodríguez, S., Querol, X., Alastuey, A., and Plana, F.: Sources and processes affecting levels and composition of atmospheric aerosol in the western Mediterranean, Journal of Geophysical Research: Atmospheres, 107, 1–14, doi:10.1029/2001JD001488, 2002.

Rodríguez, S., Querol, X., Alastuey, A., and de la Rosa, J.: Atmospheric particulate matter and air quality in the Mediterranean: A review, Environmental Chemistry Letters, 5, 1–7, doi:10.1007/s10311-006-0071-0, 2007.

Röösli, M., Theis, G., Künzli, N., Staehelin, J., Mathys, P., Oglesby, L., Camenzind, M., and Braun-Fahrländer, C.: Temporal and spatial variation of the chemical composition of PM10 at urban and rural sites in the Basel area, Switzerland, Atmospheric Environment, 35, 3701–3713, doi:10.1016/S1352-2310(00)00511-2, 2001.

Royer, P., Raut, J., Ajello, G., Berthier, S., and Chazette, P.: Synergy between CALIOP and MODIS instruments for aerosol monitoring: Application to the Po Valley, Atmospheric Measurement Techniques, 3, 893–907, doi:10.5194/amt-3-893-2010, 2010.

Salameh, D., Detournay, A., Pey, J., Pérez, N., Liguori, F., Saraga, D., Bove, M. C., Brotto, P., Cassola, F., Massabò, D., Latella, A., Pillon, S., Formenton, G., Patti, S., Armengaud, A., Piga, D., Jaffrezo, J. L., Bartzis, J., Tolis, E., Prati, P., Querol, X., Wortham, H., and Marchand, N.: PM2.5 chemical composition in five European Mediterranean cities: A 1-year study, Atmospheric Research, 155, 102–117, doi:10.1016/j.atmosres.2014.12.001, http://dx.doi.org/10.1016/j.atmosres.2014.12.001, 2015.

Salvador, R., Calbó, J., and Millán, M. M.: Horizontal Grid Size Selection and its Influence on Mesoscale Model Simulations, Journal of Applied Meteorology, 38, 1311–1329, doi:10.1175/1520-

Atmospheric
Chemistry
and Physics
Discussions

0450(1999)038<1311:HGSSAI>2.0.CO;2, http://journals.ametsoc.org/doi/abs/10.1175/1520-0450(1999)
038{\T1\textless}1311:HGSSAI{\T1\textgreater}2.0.CO;2, 1999.

Scheeren, H. A., Lelieveld, J., Roelofs, G. J., Williams, J., Fischer, H., de Reus, M., de Gouw, J. A., Warneke,
C., Holzinger, R., Schlager, H., Klüpfel, T., Bolder, M., van der Veen, C., and Lawrence, M.: The impact of
monsoon outflow from India and Southeast Asia in the upper troposphere over the eastern Mediterranean, At-
mos. Chem. Phys., 3, 1589–1608, doi:10.5194/acp-3-1589-2003, http://www.atmos-chem-phys.net/3/1589/
2003/http://www.atmos-chem-phys.net/3/1589/2003/acp-3-1589-2003.pdf, 2003.

Sciare, J., Cachier, H., Oikonomou, K., Ausset, P., Sarda-Estève, R., and Mihalopoulos, N.: Characterization
of carbonaceous aerosols during the MINOS campaign in Crete, July–August 2001: a multi-analytical ap-
proach, Atmos. Chem. Phys., 3, 1743–1757, doi:10.5194/acp-3-1743-2003, http://www.atmos-chem-phys.
net/3/1743/2003/http://www.atmos-chem-phys.net/3/1743/2003/acp-3-1743-2003.pdf, 2003.

Sciare, J., Oikonomou, K., Favez, O., Markaki, Z., Liakakou, E., Cachier, H., and Mihalopoulos, N.: Long-term
measurements of carbonaceous aerosols in the eastern Mediterranean: evidence of long-range transport of
biomass burning, Atmospheric Chemistry and Physics, 8, 5551–5563, doi:10.5194/acpd-8-6949-2008, 2008.

Sellegri, K., Pey, J., Rose, C., Culot, A., DeWitt, H. L., Mas, S., Schwier, A. N., Temime-Roussel, B., Charriere,
B., Saiz-Lopez, A., Mahajan, A. S., Parin, D., Kukui, A., Sempere, R., D'Anna, B., and Marchand, N.:
Evidence of atmospheric nanoparticle formation from emissions of marine microorganisms, Geophysical
Research Letters, 43, 6596–6603, doi:10.1002/2016GL069389, 2016.

Silva, P. and Prather, K.: On-Line Characterization of Individual Particles from Automobile Emissions, En-
vironmental Science & Technology, 31, 3074–3080, doi:10.1021/es961063d, http://pubs.acs.org/doi/abs/10.
1021/es961063d, 1997.

Silva, P., Liu, D.-Y. D.-Y., Noble, C., and Prather, K.: Size and Chemical Characterization of Individual Par-
ticles Resulting from Biomass Burning of Local Southern California Species, Environmental Science &
Technology, 33, 3068–3076, doi:10.1021/es980544p, http://pubs.acs.org/doi/abs/10.1021/es980544p, 1999.

Silva, P., Carlin, R., and Prather, K.: Single particle analysis of suspended soil dust from Southern California,
Atmospheric Environment, 34, 1811–1820, doi:10.1016/S1352-2310(99)00338-6, http://linkinghub.elsevier.
com/retrieve/pii/S1352231099003386, 2000.

Silva, P. J. and Prather, K. A.: Interpretation of Mass Spectra from Organic Compounds in Aerosol Time-of-
Flight Mass Spectrometry, Analytical Chemistry, 72, 3553–3562, doi:10.1021/ac9910132, http://www.ncbi.
nlm.nih.gov/pubmed/10952542http://pubs.acs.org/doi/abs/10.1021/ac9910132, 2000.

Song, X., Klaas, N., Faber, M., Hopke, P., Suess, D., Prather, K., Schauer, J., and Cass, G.: Source apportion-
ment of gasoline and diesel by multivariate calibration based on single particle mass spectral data, Analytica
Chimica Acta, 446, 329–343, doi:10.1016/S0003-2670(01)01270-3, 2001.

Soriano, C., Baldasano, J., Buttler, W., and Moore, K.: Circulatory patterns of air pollutants within the Barcelona
air basin in a summertime situation: lidar and numerical approaches, Boundary-Layer Meteorology, 98, 33–
55, doi:10.1023/A:1018726923826, http://link.springer.com/article/10.1023/A:1018726923826, 2001.

Sorooshian, A., Padro, L., Nenes, A., Feingold, G., McComiskey, A., Hersey, S., Gates, H., Jonsson, H., Miller,
S., Stephens, G., Flagan, R., and Seinfeld, J.: On the link between ocean biota emissions, aerosol, and mar-
itime clouds: Airborne, ground, and satellite measurements off the coast of California, Global Biogeochem-
ical Cycles, 23, 1–15, doi:10.1029/2009GB003464, 2009.

Atmospheric
Chemistry
and Physics
Discussions

Spencer, M. and Prather, K.: Using ATOFMS to Determine OC/EC Mass Fractions in Particles, Aerosol Science & Technology, 40, 585–594, doi:10.1080/02786820600729138, http://www.informaworld.com/openurl?genre=article{&}doi=10.1080/02786820600729138{&}magic=crossref||D404A21C5BB053405B1A640AFFD44AE3, 2006.

1155   Spencer, M., Holecek, J., Corrigan, C., Ramanathan, V., and Prather, K.: Size-resolved chemical composition of aerosol particles during a monsoonal transition period over the Indian Ocean, Journal of Geophysical Research, 113, 1–14, doi:10.1029/2007JD008657, http://www.agu.org/pubs/crossref/2008/2007JD008657.shtml, 2008.

Steele, P., Srivastava, A., Pitesky, M., Fergenson, D., Tobias, H., Gard, E., and Frank, M.: Desorption/ionization
1160   fluence thresholds and improved mass spectral consistency measured using a flattop laser profile in the bioaerosol mass spectrometry of single Bacillus endospores, Analytical Chemistry, 77, 7448–7454, doi:10.1021/ac051329b, 2005.

Su, Y., Sipin, M., Furutani, H., and Prather, K.: Development and Characterization of an Aerosol Time-of-Flight Mass Spectrometer with Increased Detection Efficiency, Analytical Chemistry, 76, 712–719,
1165   doi:10.1029/2001JD001211.(12), http://pubs.acs.org/doi/abs/10.1021/ac034797z, 2004.

Sullivan, R. and Prather, K.: Investigations of the diurnal cycle and mixing state of oxalic acid in individual particles in Asian aerosol outflow., Environmental Science & Technology, 41, 8062–9, doi:10.1021/es071134g, http://www.ncbi.nlm.nih.gov/pubmed/18186338, 2007.

Sullivan, R., Guazzotti, S., Sodeman, D., and Prather, K.: Direct observations of the atmospheric processing
1170   of Asian mineral dust, Atmospheric Chemistry and Physics, 7, 1213–1236, doi:10.5194/acp-7-1213-2007, http://www.atmos-chem-phys.net/7/1213/2007/, 2007.

Tao, S., Wang, X., Chen, H., Yang, X., Li, M., Li, L., and Zhou, Z.: Single particle analysis of ambient aerosols in Shanghai during the World Exposition, 2010: two case studies, Frontiers of Environmental Science & Engineering in China, 5, 391–401, doi:10.1007/s11783-011-0355-x, http://link.springer.com/10.
1175   1007/s11783-011-0355-x, 2011.

Turnbull, A. and Harrison, R.: Major component contributions to PM10 composition in the UK atmosphere, Atmospheric Environment, 34, 3129–3137, doi:10.1016/S1352-2310(99)00441-0, 2000.

Wang, X., Ye, X., Chen, H., Chen, J., Yang, X., and Gross, D. S.: Online hygroscopicity and chemical measurement of urban aerosol in Shanghai, China, Atmospheric Environment, 95, 318–326,
1180   doi:10.1016/j.atmosenv.2014.06.051, http://dx.doi.org/10.1016/j.atmosenv.2014.06.051, 2014.

Wenzel, R. and Prather, K.: Improvements in ion signal reproducibility obtained using a homogeneous laser beam for on-line laser desorption/ionization of single particles, Rapid Communications in Mass Spectrometry, 18, 1525–1533, doi:10.1002/rcm.1509, http://www.ncbi.nlm.nih.gov/pubmed/15216516, 2004.

Whiteaker, J. and Prather, K.: Hydroxymethanesulfonate as a tracer for fog processing of individual aerosol par-
1185   ticles, Atmospheric Environment, 37, 1033–1043, doi:10.1016/S1352-2310(02)01029-4, http://linkinghub.elsevier.com/retrieve/pii/S1352231002010294, 2003.

Willis, M. D., Burkart, J., Thomas, J. L., Köllner, F., Schneider, J., Bozem, H., Hoor, P. M., Aliabadi, A. A., Schulz, H., Herber, A. B., Leaitch, W. R., and Abbatt, J. P. D.: Growth of nucleation mode particles in the summertime Arctic: A case study, Atmospheric Chemistry and Physics, 16, 7663–7679, doi:10.5194/acp-
1190   16-7663-2016, 2016.

Wyslouzil, B. E., Seinfeld, J. H., Flagan, R. C., and Okuyama, K.: Binary nucleation in acid–water systems. I. Methanesulfonic acid–water, The Journal of Chemical Physics, 94, 6827, doi:10.1063/1.460261, http://scitation.aip.org/content/aip/journal/jcp/94/10/10.1063/1.460261, 1991a.

Wyslouzil, B. E., Seinfeld, J. H., Flagan, R. C., and Okuyama, K.: Binary nucleation in acid–water systems. II. Sulfuric acid–water and a comparison with methanesulfonic acid–water, The Journal of Chemical Physics, 94, 6842, doi:10.1063/1.460262, http://scitation.aip.org/content/aip/journal/jcp/94/10/10.1063/1.460261http://scitation.aip.org/content/aip/journal/jcp/94/10/10.1063/1.460262, 1991b.

Yang, F., Chen, H., Wang, X., Yang, X., Du, J., and Chen, J.: Single particle mass spectrometry of oxalic acid in ambient aerosols in Shanghai: Mixing state and formation mechanism, Atmospheric Environment, 43, 3876–3882, doi:10.1016/j.atmosenv.2009.05.002, http://linkinghub.elsevier.com/retrieve/pii/S1352231009004154, 2009.

Yu, J. Z., Huang, X.-F., Xu, J., and Hu, M.: When aerosol sulfate goes up, so does oxalate: implication for the formation mechanisms of oxalate., Environmental science & technology, 39, 128–133, doi:10.1021/es049559f, 2005.

Zhang, Q., Jimenez, J. L., Canagaratna, M. R., Ulbrich, I. M., Ng, N. L., Worsnop, D. R., and Sun, Y.: Understanding atmospheric organic aerosols via factor analysis of aerosol mass spectrometry: A review, Analytical and Bioanalytical Chemistry, 401, 3045–3067, doi:10.1007/s00216-011-5355-y, 2011.

Zhang, Y., Wang, X., Chen, H., Yang, X., Chen, J., and Allen, J.: Source apportionment of lead-containing aerosol particles in Shanghai using single particle mass spectrometry., Chemosphere, 74, 501–7, doi:10.1016/j.chemosphere.2008.10.004, http://www.ncbi.nlm.nih.gov/pubmed/19027137, 2009.

Zhu, S., Sartelet, K. N., Healy, R. M., and Wenger, J. C.: Simulation of particle diversity and mixing state over Greater Paris: a model– measurement inter-comparison, Faraday Discuss. Faraday Discuss, 189, 547–566, doi:10.1039/c5fd00175g, http://dx.doi.org/10.1039/C5FD00175G, 2016.

Atmospheric
Chemistry
and Physics
Discussions

Table 1. List of instruments deployed at Cap Corsica during the ADRIMED and SAF-MED field campaigns. See text for instrument acronym details.

Parameter	Instrument	Make & Model	Temporal resolution	Institution
Particle number size distribution (10-500 nm, mobility diameter and 300 nm − 20 µm, optical diameter)	SMPS	TSI Instruments Ltd., DMA model 3080 and CPC model 3010	5 min (continuous)	CNRM GAME
	OPS	TSI Instruments Ltd., model 3300	5 min (continuous)	CNRM GAME
PM_{10} and PM_1 mass concentration	TEOM, TEOM-FDS		continuous	LSCE
Chemical composition and size distribution of non-refractory and refractory particles (100-3000 nm, vacuum aerodynamic diameter)	ATOFMS	TSI Instruments Ltd., model 3800-100	continuous	UCC
Chemical composition of non-refractory particles (30-1000 nm, vacuum aerodynamic diameter)	ACSM	Aerodyne Research Inc.	25 min (continuous)	LSCE
Black carbon (BC), $PM_{2.5}$	MAAP	Thermo-Scientific, model 5012	5 min (continuous)	LSCE
PM_{10} chemical composition (Na^+, Mg^+, Cl^-, Ca^{2+}, K^+, NH_4^+, NO_2^-, SO_4^{2-}, MSA, Oxalate)	PILS-IC		12/18 min (continuous)	LSCE
Pressure, temperature, relative humidity, solar radiation, rain, wind speed and direction	Weather station	Campbell Scientific, Model CR1000	5 min (continuous)	LSCE

Table 2. Detailed composition of ATOFMS dataset during ADRIMED and SAF-MED, by particle classes.

Category	Particle Class	No. of Particles	% of Total Ionised	% Particles with negative spectra	No. of Particles containing Oxalate	No. of Particles containing MSA	Assumed Density (g/cm³)	% of Total ATOFMS Mass	Unscaled Peak Aerodynamic Diameter (µm)
EC	EC-SOx	329555	28	3			1.4	22	0.74
	EC-Oxalate	15462	1	0.5			1.4	1	0.72
	EC-K	40666	3	16	222		1.4	4	0.76
	EC-K-SOx	13627	1	76		445	1.4	5	0.74
	EC-K-Oxalate	23399	2	0.3			1.4	1	0.74
	K-EC-NOx	1391	0.1	100			1.4	7	0.74
	K-EC-SOx	57553	5	100		191	1.4	4	0.85
	K-EC-Oxalate	161225	13	0.3			1.4	7	0.74
K-rich	K-CN	41740	3	35			1.8	17	0.76
	K-NOx	12078	1	100	3118		1.8	1	0.91
	K-SOx	296512	25	9		782	1.8	3	0.85
	K-SOx-Oxalate	28754	2	100	4988		1.8	2	0.97
	K-Aluminosilicate	3797	0.3	21	23		2	2	0.91
	K-Na	2500	0.2	14			2	1	0.79
Na-rich	Sea salt-fresh	26175	2	68			2.2	6	1.54
	Sea salt-aged	69566	6	59	270		2.2	3	1.81
	Na-EC	1415	0.1	100			2.2	3	0.59
Amines	K-TMA	25603	2	0			1.5	1	0.74
	TMA-EC	19688	2	0.3			1.5	1	0.78
	OC-TMA	3734	0.3	18			1.5	0.5	0.70
OC-rich	OC	13323	1	2	110		1.8	2	0.74
	K-OC-NOx	1368	0.1	100			1.8	0.2	0.66
	K-OC-SOx	7435	1	95			1.8	1	0.64
V-rich	V	9810	1	9	71	65	3.1	2	0.70
	EC-V	3827	0.3	43		198	3.1	1	0.69
Fe-rich	Fe	2199	0.2	71	215	37	3.6	0.5	0.88
Ca-rich	Ca	2400	0.2	82	352	14	2.6	1	1.08

Atmospheric
Chemistry
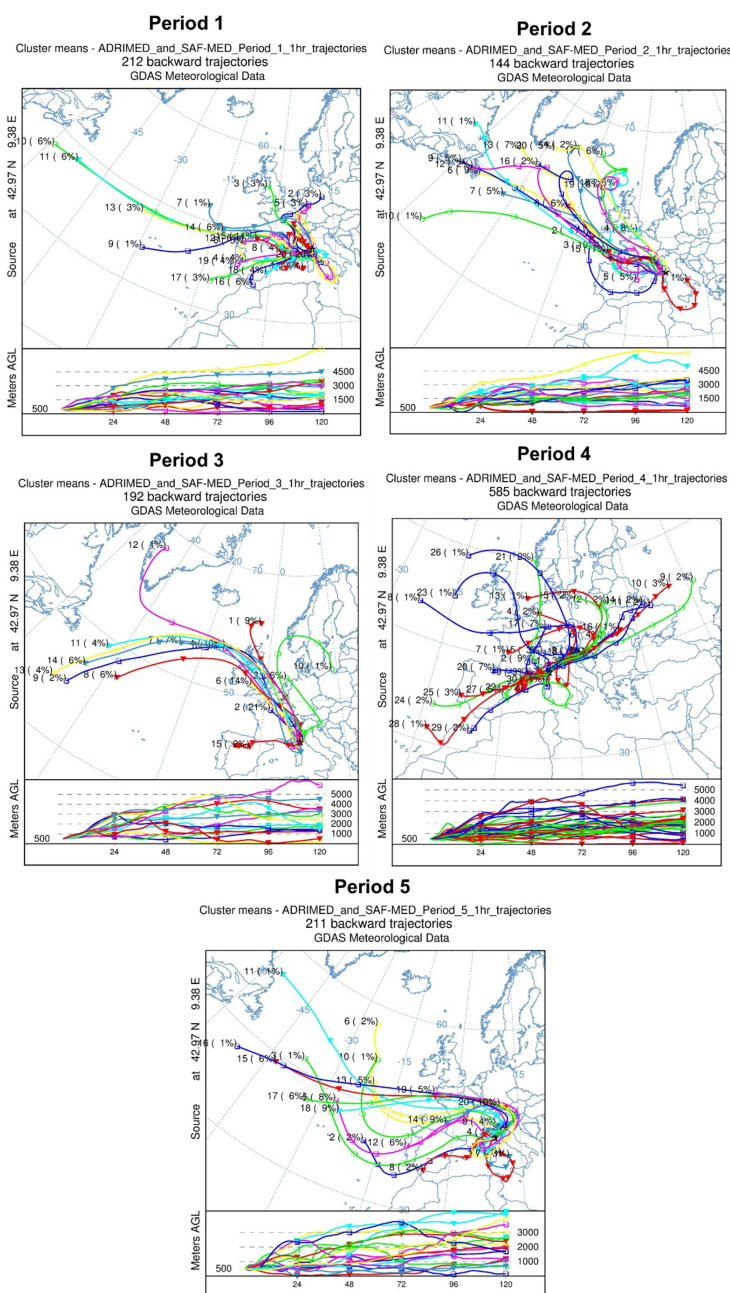and Physics
Discussions

Figure 1. Cluster analysis of 120-hour back trajectories calculated using the HYPLSIT model, ending at Cap Corse sampling site at 500 meters above ground level, every 1 hour, for the five periods identified during ADRIMED and SAF-MED.
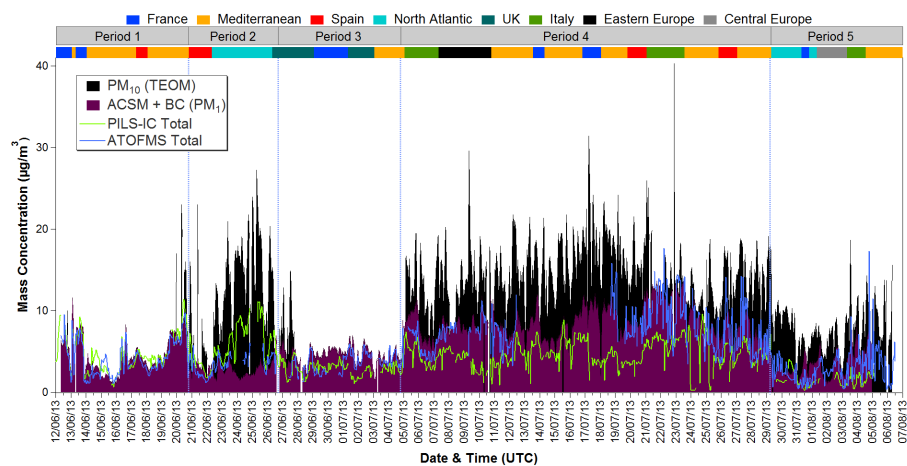
Atmospheric
Chemistry
and Physics
Discussions

Figure 2. Hourly mass concentrations of PM$_{10}$, total ACSM species + BC (PM$_1$), total PILS-IC species (PM$_{10}$) and total ionised ATOFMS particles during ADRIMED and SAF-MED.
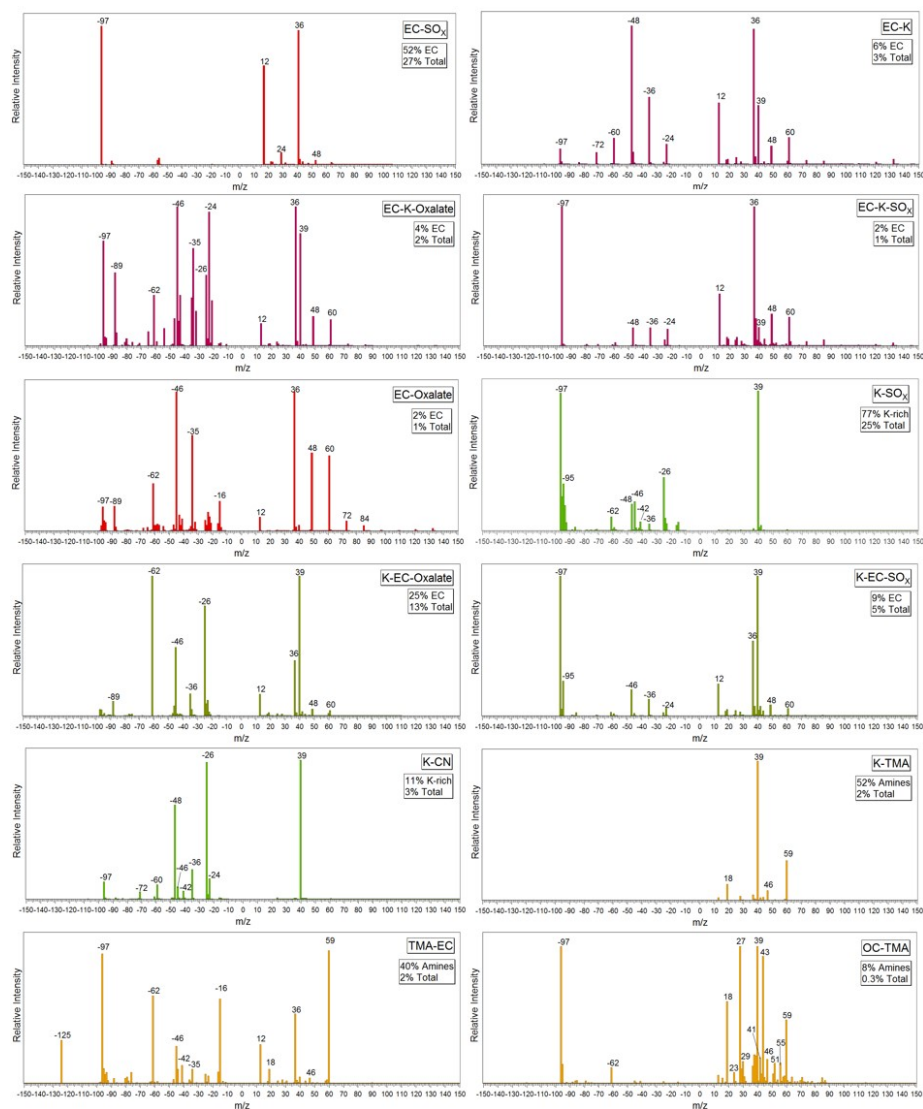
Figure 3. Average mass spectra of ATOFMS particle classes originating from regionally transported combustion sources during ADRIMED and SAF-MED. Percentages refer to fraction of ATOFMS category and total particle numbers.
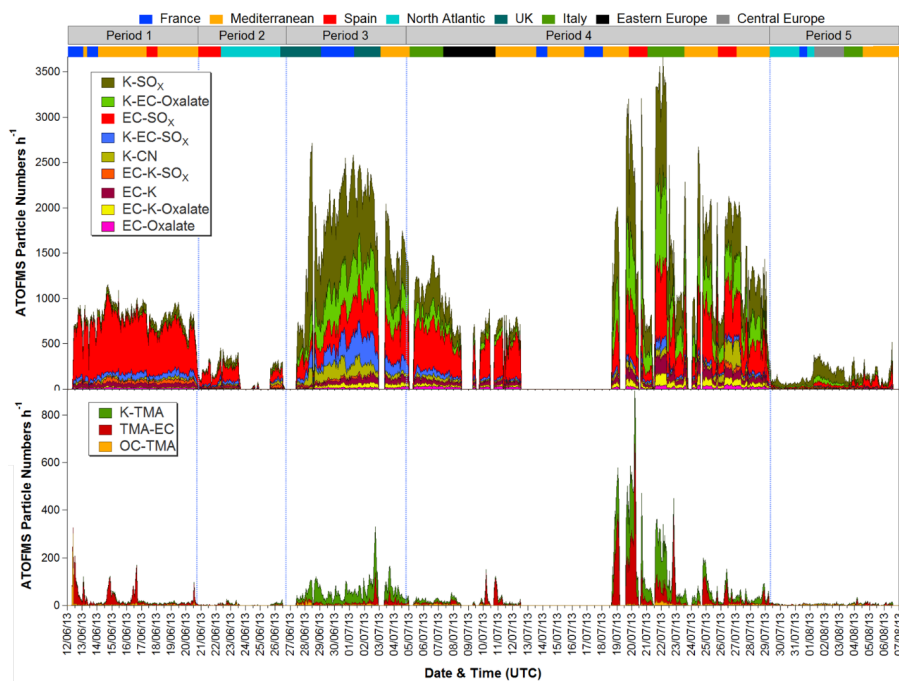
Figure 4. Time series (stacked) of hourly unscaled particle numbers for ATOFMS EC and major K-rich particle classes (top) and Amine classes (bottom) observed during ADRIMED and SAF-MED.

Figure 5. Locations of fires detected by the MODIS sensor on board the Terra and Aqua satellites over 10-day periods during ADRIMED and SAF-MED. Each red dot indicates a location where at least one fire was detected. (http://lance-modis.eosdis.nasa.gov/cgi-bin/imagery/firemaps.cgi)

Atmospheric
Chemistry
and Physics
Discussions

Open Access
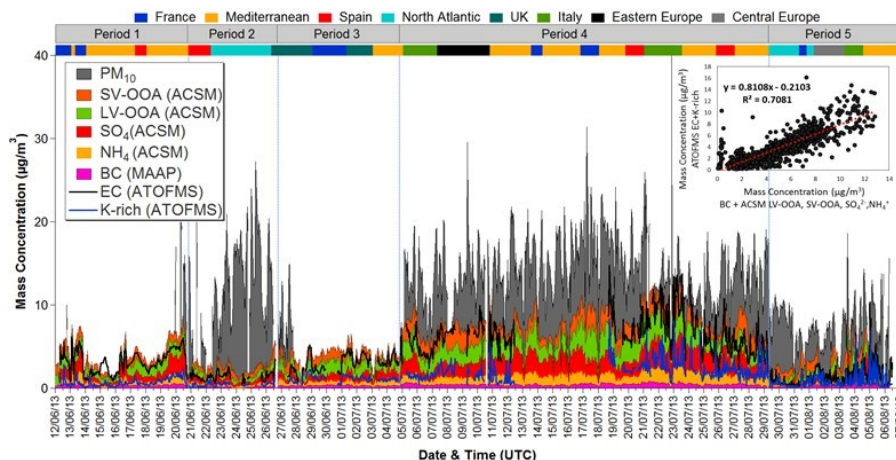
Figure 6. Hourly mass concentrations of PM_{10}, ACSM species (SO_4^{2-}, NH_4^+, organic aerosol factors SV-OOA and LV-OOA), BC and reconstructed ATOFMS EC and K-rich particles. BC and ACSM species profiles are stacked, as are both ATOFMS categories, but separately. This compares the ATOFMS mass concentrations with BC+ACSM species. Inset is a scatter plot of mass concentrations of ATOFMS EC-rich+K-rich particles compared with those for BC+SV-OOA+LV-OOA+SO_4^{2-}+NH_4^+.
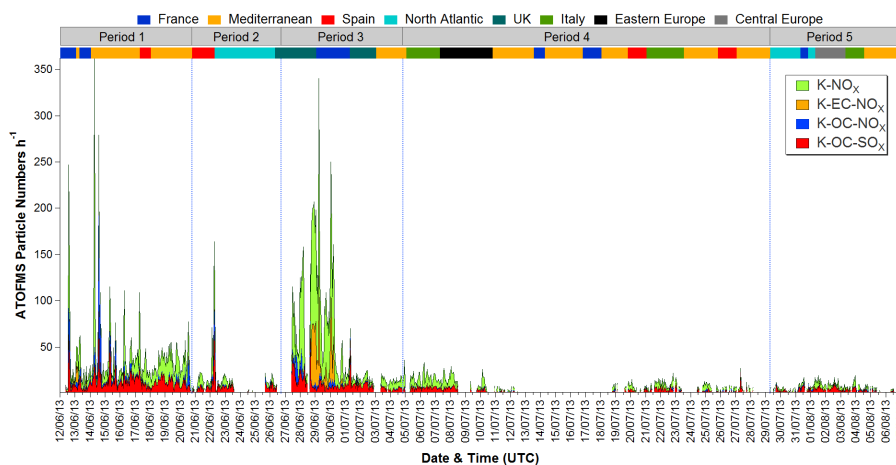
Figure 7. Time series of hourly unscaled particle numbers for ATOFMS particle classes associated with local biomass burning observed during ADRIMED and SAF-MED.
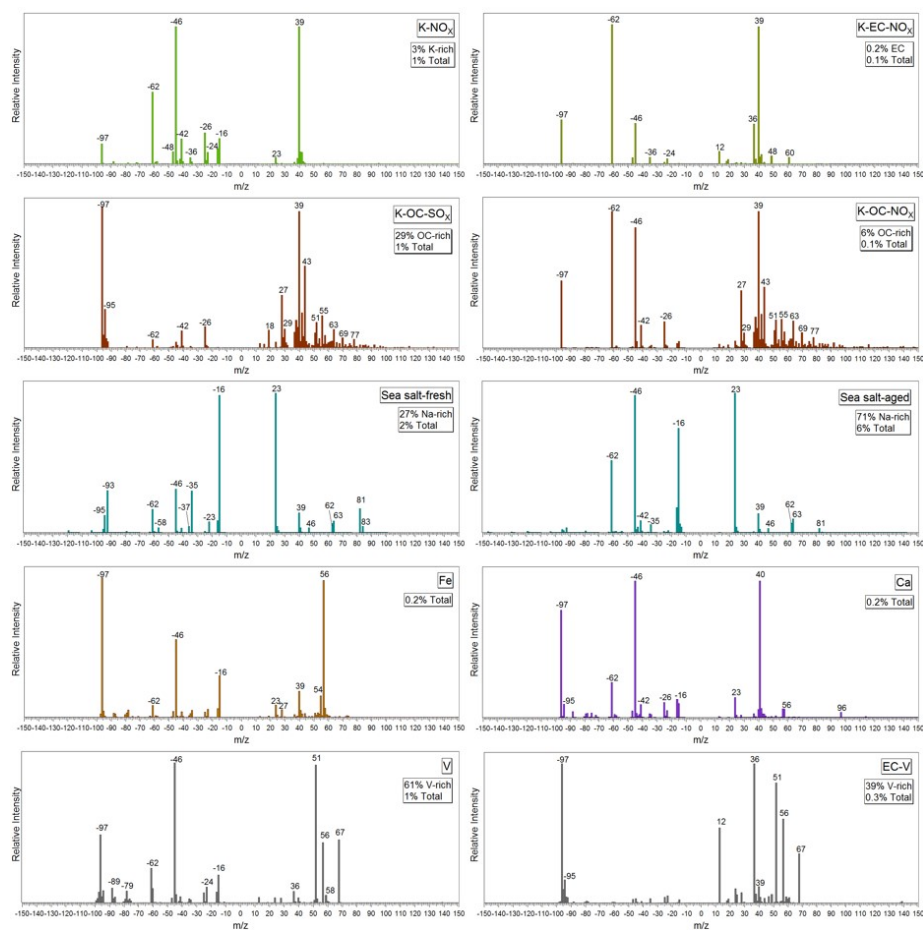
Atmospheric
Chemistry
and Physics
Discussions

Figure 8. Average mass spectra for ATOFMS particle classes from local biomass burning, marine, dust and shipping sources during ADRIMED and SAF-MED.
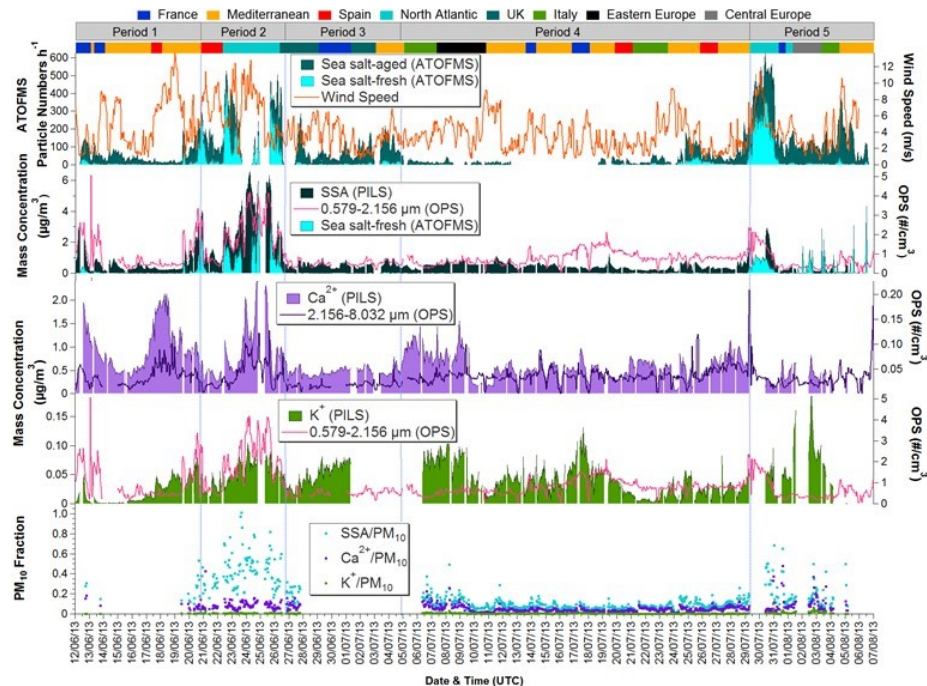
Atmospheric
Chemistry
and Physics
Discussions

Figure 9. Time series of hourly ATOFMS sea salt particle numbers, OPS number concentrations, PILS-IC SSA (sea salt aerosol), Ca^+, K^+ and ATOFMS fresh sea salt mass concentrations, and PM_{10} fractions observed during ADRIMED and SAF-MED.
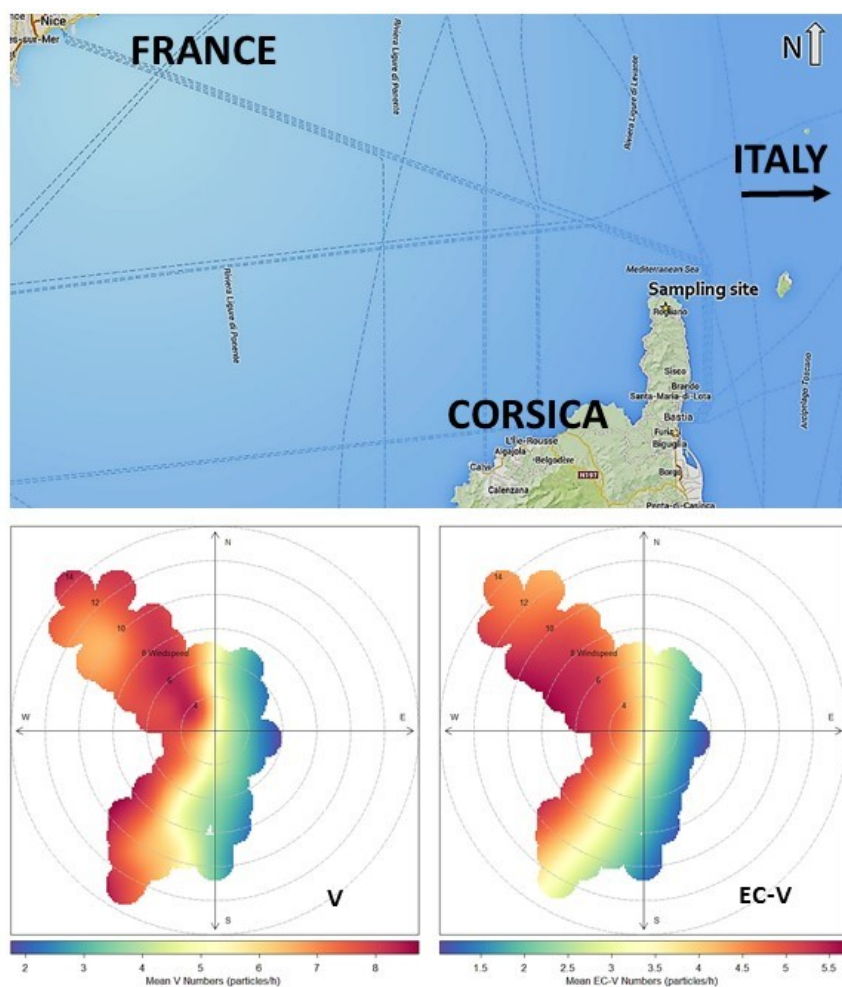
Atmospheric
Chemistry
and Physics
Discussions

Figure 10. Passenger ferry lanes around the sampling site on Corsica (top) and wind speed and direction dependences (bottom) for ATOFMS V-rich particles observed during ADRIMED and SAF-MED.
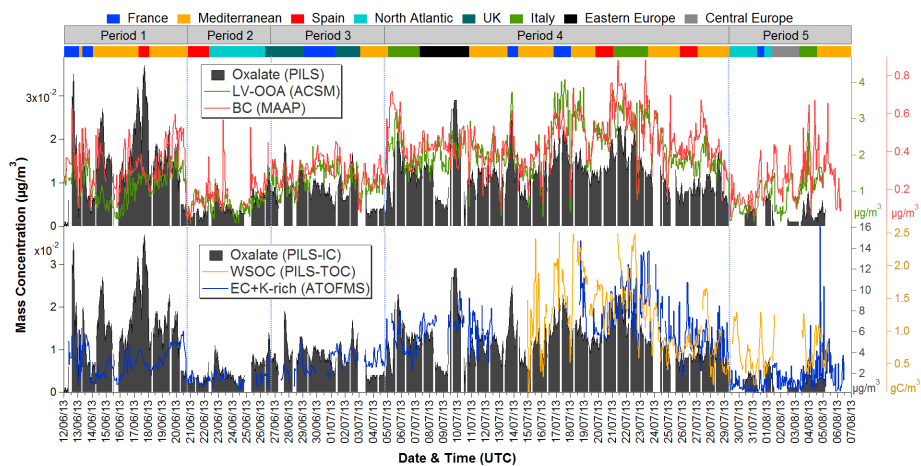
Atmospheric
Chemistry
and Physics
Discussions

Figure 11. Hourly mass concentrations of the ACSM factor SV-OOA, BC (black carbon), WSOC (water soluble organic carbon) and ATOFMS EC+K-rich particles during ADRIMED and SAF-MED.
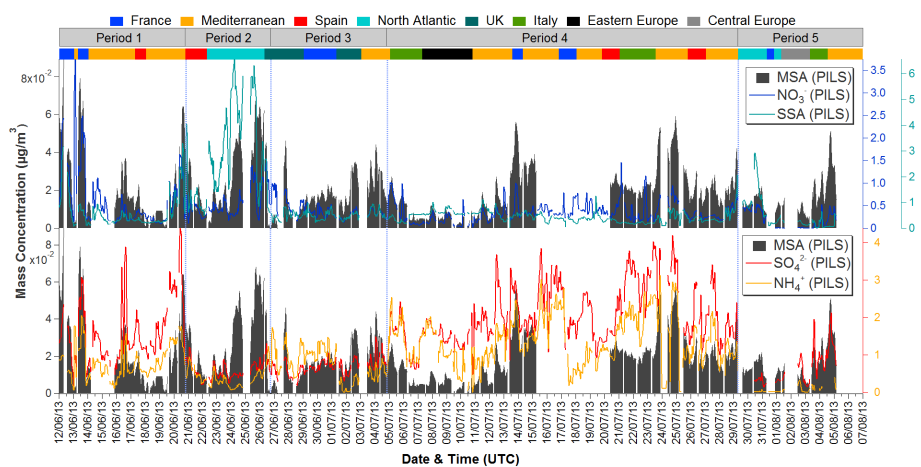

Figure 12. Hourly mass concentrations of PILS-IC species MSA (methanesulfonate), NO_3^-, SSA (sea salt aerosol), SO_4^{2-} and NH_4^+ during ADRIMED and SAF-MED.